AWARD NUMBER: **W81XWH-20-1-0048**

TITLE: **Fusogen Nanomedicine for Peripheral Nerve Repair**

PRINCIPAL INVESTIGATOR: **Wise Young, MD, PhD**

CONTRACTING ORGANIZATION: **Rutgers University, New Brunswick, NJ**

REPORT DATE: **January 2023**

TYPE OF REPORT: **Annual**

PREPARED FOR: U.S. Army Medical Research and Development Command
Fort Detrick, Maryland 21702-5012

REPORT DOCUMENTATION PAGE

Form Approved
OMB No. 0704-0188

1. REPORT DATE	2. REPORT TYPE	3. DATES COVERED
January 2023	Annual	01Jan2022-31Dec2022

4. TITLE AND SUBTITLE

Fusogen Nanomedicine for Peripheral Nerve Repair

5a. CONTRACT NUMBER
W81XWH-20-1-0048

5b. GRANT NUMBER

5c. PROGRAM ELEMENT NUMBER

6. AUTHOR(S) David I Devore, PhD; Cemile Bektas, PhD; Daniel Chakhalian, MD; Kim-phuong Le, PhD; Mariana Lima, BS; Yong Mao, PhD; Antonio Merolli, MD; Joseph M Rosen, MD, Dongming Sun, PhD, Wise Young, MD PhD

E-Mail:wisey@dls.rutgers.edu

5d. PROJECT NUMBER

5e. TASK NUMBER

5f. WORK UNIT NUMBER

7. PERFORMING ORGANIZATION NAME(S) AND ADDRESS(ES)
Rutgers, the State University of New Jersey

8. PERFORMING ORGANIZATION REPORT NUMBER

9. SPONSORING / MONITORING AGENCY NAME(S) AND ADDRESS(ES)

U.S. Army Medical Research and Development Command
Fort Detrick, Maryland 21702-5012

10. SPONSOR/MONITOR'S ACRONYM(S)

11. SPONSOR/MONITOR'S REPORT NUMBER(S)

12. DISTRIBUTION / AVAILABILITY STATEMENT
Approved for Public Release; Distribution Unlimited

13. SUPPLEMENTARY NOTES

14. ABSTRACT This project is directed at the PRMRP Focus Area of ***development of novel therapies to repair neurosensory damage.*** The project deliverables are **fusogenic nanoparticles (FNPs),** comprised of polymeric fusogens (biomaterials that enhance cell membrane fusion) and cholesterol, to synergistically repair injured peripheral nerves. ***The central hypothesis*** being tested is that structure-function relationships among novel amphiphilic **tyrosine-derived block copolymer surfactants (TyPS)** can lead to effective FNPs which will allow immediate re-establishment of axonal continuity and function. This is being enabled by the first thermodynamically-based systematic exploration of structure-activity relations for polymeric fusogens. Concurrently, **controlled delivery of cholesterol**, a natural membrane component with fusogenic properties which is being encapsulated in the TyPS-based FNPs, is for the first time being investigated for repair of severed nerves. ***The rationale*** for this project is that, after injuries involving the transection of nerves, anatomical recovery is usually incomplete due to inherently slow nerve regrowth rates and rapid proximal and distal (Wallerian) degeneration of the stumps. Consequently, patients can suffer substantial life-long disability and even chronic pain if a neuroma follows. Among combat wounded US military personnel, nerve injuries are a leading cause of unfitting conditions and each year over 100,000 civilian trauma patients suffer disabling nerve injuries which incur enormous long-term healthcare costs. There are currently no fusogens useful for nerve repair approved by the US Food and Drug Administration.

15. SUBJECT TERMS None listed.

16. SECURITY CLASSIFICATION OF:			17. LIMITATION OF ABSTRACT	18. NUMBER OF PAGES	19a. NAME OF RESPONSIBLE PERSON
a. REPORT	b. ABSTRACT	c. THIS PAGE			USAMRDC
Unclassified	Unclassified	Unclassified	Unclassified	40	19b. TELEPHONE NUMBER *(include area code)*

Table of Contents

1. INTRODUCTION: ***5***

2. KEYWORDS: ***5***

3. ACCOMPLISHMENTS: ***5***

Specific Aim 1: Formulation and biophysical properties of Fusogen Nanoparticles (FNPs) **8**

Task 1. Design and synthesis of tyrosine-derived block copolymer surfactants (TyPS). 8

Task 2. Biophysical properties of TyPS. 13

Task 3. Biophysical properties of Fusogen Nanoparticles (FNPs) 19

Task 4. IACUC and ACURO animal protocol reviews 22

Specific Aim 2: Evaluation of functional nanoparticle (FNP) *in vitro* axonal membrane repair and cytotoxicity **22**

Task 5: FNP repair of dorsal root ganglion (DRG) axon membranes. 22

Task 6. Cytotoxicity of Fusogen Nanoparticles (FNPs) 24

Specific Aim 3: Evaluation of the lead FNP in an in vivo rat tibial nerve injury model. **27**

4. IMPACT: ***30***

5. CHANGES/PROBLEMS: ***32***

6. PRODUCTS: ***33***

7. PARTICIPANTS & OTHER COLLABORATING ORGANIZATIONS ***35***

8. SPECIAL REPORTING REQUIREMENTS ***38***

9. APPENDICES: ***39***

Appendix 1. Quad Chart **39**

Appendix 2. Transition Plan Questionnaire **40**

1. INTRODUCTION:

Nerve damage, including crushed and severed nerves, is one of the most frequent and debilitating injuries suffered in combat as well as in civilian trauma cases. Current methods of nerve repair include surgical suturing (direct end-to-end coaptation) or nerve grafts depending on the injury gap distance between distal and proximal nerve stumps. In either case, axonal regeneration is a slow process and functional recovery is dependent on the site of injury and the type of treatment, being slow, poor or absent in the worst cases. Several polymers such as poly(ethylene glycol) (PEG) have been found to act as fusogens (defined as biomaterials which enhance the fusion of cell membrane). The proposed research will, for the first time, provide a thermodynamically-based systematic exploration of structure-activity relations for polymeric fusogens comprised of synthetically tunable tyrosine-derived polymeric surfactants (TyPSs). The controlled delivery of cholesterol with TyPS-based fusogen nanoparticles (FNPs) will also, for the first time, be investigated for the repair of axonal membranes. The FNPs will then be applied to in vivo nerve repair to better characterize the relationship between fusogenicity and electrophysiological and histological outcomes.

2. KEYWORDS:

fusogens; peripheral nerve repair; tyrosine-derived polymeric surfactants; cholesterol; nanoparticles; hydrophile:lipophile balance; cytotoxicity; hemolysis; dorsal root ganglia

3. ACCOMPLISHMENTS:

What were the major goals of the project?

The study design consists of three Specific Aims. In **Aim 1, Formulation and biophysical properties of FNPs,** diblock and triblock tyrosine-derived polymeric surfactants (TyPSs) have been designed and synthesized based on calculated thermodynamic properties (hydrophile-lipophile balance (HLB) and Hildebrandt-Hansen solubility parameters), evaluated for insertion in model phospholipid membranes and formulated into self-assembled TyPS-cholesterol fusogen nanoparticles (FNPs) which have been characterized for particle size and cholesterol binding levels. In **Aim 2, Evaluation of FNP in vitro axonal membrane repair and cytotoxicity,** a fluorochrome dynamics methods has been developed to measure axon fusion in severed rat dorsal root ganglia (DRG) membranes treated with the FNPs, PEG and Poloxamer 188; TyPS were demonstrated to be non-cytotoxic to human dermal microvascular endothelial cells; and, flow cytometry was used to demonstrate improved cell viability with rat B35 neuroblastoma cells. In **Aim 3, Evaluation of the lead FNP in an in vivo rat tibial (sciatic - tibial branch) nerve injury model,** the US Army Animal Care and Use Review Office (ACURO) has approved our protocol for the in vivo evaluation of the FNPs for repair of severed tibial nerves, with electrophysiological and histological outcomes used to determine the relative treatment efficacies of the known fusogens poly(ethylene glycol) (PEG) and Poloxamer 188 (a commercial block copolymer surfactant) and the selected FNP injected at the surgical site. The status of the tasks and milestones in the Statement of Work are summarized in the table below.

Specific Aim 1: Formulation and biophysical properties of Fusogen Nanoparticles (FNPs)	Timeline Months	Status
Major Task 1: Design and synthesis of tyrosine-derived block copolymer surfactants (TyPSs)	1-2	
Subtask 1.1: Thermodynamic calculations of Hoy solubility parameters and Hydrophile:Lipophile Balances (HLBs) for TyPSs over the statistically designed parameter ranges	1-2	100% Complete
Subtask1 2: Synthesis and structural characterization of a library of 16 initial TyPSs	1-2	50% complete
Milestone: TyPSs' compositions confirmed by ^{1}H NMR and GPC	2	100% complete
Major Task 2: Biophysical properties of TyPSs	3-5	
Subtask 2.1: Determine surface tensions and critical aggregation concentrations (CACs) of TyPSs in PBS	3-4	50% Complete
Subtask 2.2: Determine Langmuir film balance surface pressure/surface area properties for TyPS, PEG and P188 insertion in DPPC, DPPG and PS phospholipid films	4-5	80% Complete
Milestone(s): Structure-property relations determined for TyPSs based on their solubility parameters, HLBs, CACs and surface pressure/surface area responses	5	80% complete
Major Task 3: Biophysical properties of FNPs	5-8	
Subtask 3.1: Prepare self-assembled FNPs of each TyPS and cholesterol and determine particle sizes, zeta potentials and stabilities as a function of cholesterol loading/binding levels	5-6	100% complete
Subtask 3.2: Determine cholesterol release kinetics from the FNPs in PBS	6-7	100% complete
Subtask 3.3: Determine $\log_{10}$P(o/w) for the FNPs	6-7	0% complete
Milestones: Correlation of FNP properties with TyPS properties; Identification and synthesis of additional TyPS compositions based on Stat-Ease statistical design analysis for optimized FNP biophysical properties	8	50% complete
Major Task 4: IACUC and ACURO animal protocol reviews	4-12	
Subtask 4.1: Document rat tibial nerve protocol surgical procedure, animal care and safety, and	4-6	100% Complete

experimental design; submit to Rutgers IACUC and US Army ACURO		
Milestones: IACUC and ACURO approvals of rat nerve injury protocol	12	100% Complete
Specific Aim 2: **Evaluation of FNP *in vitro* axonal membrane repair and cytotoxicity.**		**Site 1**
Major Task 5: FNP repair of DRG axon membranes		
Subtask 5.1: Compare the efficacy of FNPs, PEG and P188 for fusion of severed DRG axon fusion based on fluorochrome dynamics	7-12	100% complete
Subtask 5.2: Determine the efficacy of FNPs for delivery of cholesterol to DRG axonal membranes based on quantitative HPLC analysis	12-16	0% complete
Major Task 6: Cytotoxicity of FNPs		
Subtask 6.1. Determine the cytotoxicity of FNPs, TyPSs, PEG and P188 based on MTT viability assays for HECs and primary nerve cells	14-16	100% Complete
Subtask 6.2: Determine the hemolytic activity of FNPs, TyPS, PEG and P188	14-16	0% complete
Milestone: Structure-performance relations determined for FNP repair of severed DRG axons and for cytotoxicities; Lead candidate FNP identified for Aim 3 *in vivo* studies	16	50% complete
Specific Aim 3: ***Evaluation of the lead FNP in an in vivo rat tibial nerve injury model.***		
Major Task 7: Determine relative efficacies of FNPs, PEG and P188 for repair of severed tibial nerves	17-24	
Subtask 7.1: Obtain pre-injury compound action potentials, perform surgical tibial nerve transections, inject fusogens (TyPS-cholesterol FNP, P188-cholesterol and PEG) at the surgical sites and surgically repair the nerves	17-19	0% complete
Subtask 7.2: One week post-injury, obtain post-injury compound action potentials and then euthanize the animals	20-21	0% complete

Subtask 7.3: Retrieve 20mm segments of distal and proximal tibial nerves, perform histological analysis of axon populations and conduct statistical analyses of in vivo data	21-23	0% complete
Milestones achieved: Relative fusogenic performance of FNPs and PEG determined; Final report submitted to DoD; Manuscript(s) submitted to journals; Patent applications filed	24	0% complete

What was accomplished under these goals?

The objectives, significant results and key outcomes for each of the Specific Aims and Tasks outlined in the project Statement of Work (SOW; see above Table) are provided here in the order they appear in the SOW. Most but not all of the Tasks which were targeted for completion in Year 1 of the project were fully or at least partially completed while most Year 2 Tasks were not completed due to the COVID-19 pandemic and the closure of the Kohn Lab at Rutgers University. Key Tasks will be pursued under an approved no-cost extension of the project in 2022. The project team has met biweekly since January, 2020, (initially in person and via Zoom since March, 2020) to assure collaborative planning and data reviews and will continue to do so in 2022.

To date, several key outcomes have been achieved: 1) thermodynamic solubility parameters and hydrophile;lipophile balances (HLBs) were calculated for a wide range of tyrosine-derived polymeric surfactants (TyPSs) which provided systematic estimates of TyPS ability to bind cholesterol and to interact with cell phospholipid membranes; 2) an initial set of three "A-B-A" triblock and three "A-B" diblock TyPSs were synthesized based on their predicted thermodynamic properties and were demonstrated to self-assemble into fusogen nanoparticles (FNPs) having a narrow range of diameters appropriate for injectable nanomedicines; 3) the TyPSs and the prototypical A-B-A triblock polymeric surfactant, Poloxamer 188, inserted into Langmuir phospholipid monolayer films; 4) the FNPs effectively bound significant levels of cholesterol and inserted the cholesterol into the Langmuir monolayer films; 5) the TyPS were non-cytotoxic to human dermal cells and caused the fusion of rat B35 neuroblastoma cells while improving their viability; 6) methods were advanced to investigate the end-to-end and side-to-side fusion of rat dorsal root ganglia axons but these methods have thus far not provided definitive evidence of axonal fusion caused by PEG, Poloxamer 188 or six TyPS, and, 7) the TyPS caused no significant cell fusion on a mouse fibroblast cell line but P188/PEG has a synergistic effect in promoting cell fusion.

For clarity, some parts of the Year 1, 2 Annual Report are retained here but readers are referred to that report and the attached manuscripts which have been published or submitted for publication for greater details.

Specific Aim 1: Formulation and biophysical properties of Fusogen Nanoparticles (FNPs)

Task 1. Design and synthesis of tyrosine-derived block copolymer surfactants (TyPS).

1.1. Thermodynamic property calculations.

To determine if predictive structure-property relations can be developed for polymeric fusogens, solubility parameters and surfactant properties of tyrosine-derived block copolymer surfactants

(TyPS), poly(alkylene oxides) (i.e., poly(ethylene oxide) (PEO) and poly(propylene oxide) (PPO)) and their block copolymers were calculated using established thermodynamic methods. The synthetically tunable tyrosine-derived copolymer surfactants (TyPS) were "A-B-A" triblocks and "A-B" diblocks comprised of a hydrophobic desaminotyrosyl tyrosine -diacid (DTR-XA) B-block and either one or two hydrophilic poly(ethylene oxide) A-blocks (Figure 1).[1,2,3] The thermodynamic properties were also calculated for comparable commercial triblock copolymer surfactants, known as Poloxamers™ or Pluronics™, which are comprised of PEO_n-PPO_m-PEO_n..

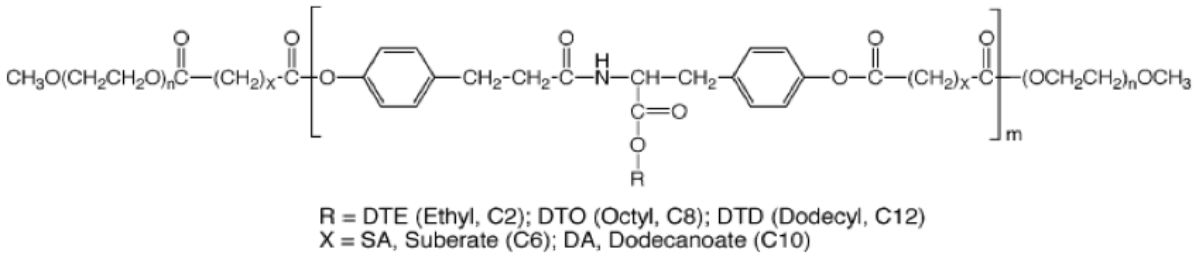

Figure 1. Tyrosine-derived block copolymer surfactant (TyPS) structure. Synthetically tunable composition variables include: the molecular weight (degree of polymerization) of the end-cap hydrophilic poly(ethylene oxide) (PEO) A-block(s) chains (n); the diacid alkyl chain length (x); the pendent alkyl ester chain length (R); and the molecular weight (degree of polymerization) of the hydrophobic oligoDTR-XA B-block (m).

Hansen solubility parameters for selected TyPS hydrophobic B-blocks, poly(ethylene oxide) (PEO), poly(propylene oxide) (PPO) and cholesterol (Figure 2) were calculated using the group contribution values of Hoftyzer and van Krevelen [4,5] and are summarized in Table 1:

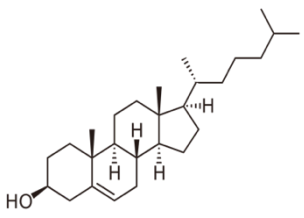

Figure 2. Cholesterol

Table 1. Calculated Hansen solubility parameters.
Solubility parameter units $(Jcm^{-3})^{1/2}$.

	∂_d	∂_p	∂_h	∂_T
DTE-SA	17.40	2.78	7.85	19.29
DTO-SA	17.40	3.44	7.11	19.11
DTD-SA	17.39	2.03	6.72	18.75
DTD-DA	17.39	1.83	6.38	18.61
PEO	17.04	10.65	8.94	21.99
PPO	15.44	5.82	8.94	17.78
Cholesterol	16.14	1.32	7.27	17.75

The solubility parameters for selected diblock and triblock TyPSs and P188 were calculated using the Hansen parameters from Table 1 and the weight fractions of the A-blocks and B-blocks, φ_a and φ_b, respectively, and were summarized in Table 2. The Flory-Huggins interaction parameters, χ, with cholesterol and with the membrane phospholipid 1,2-Dipalmitoyl-sn-glycero-3-phosphoglycerol (DPPG) were then calculated and were summarized in Table 2.

Table 2. Copolymer solubility parameters (∂_T) and Flory-Huggins interaction parameters (χ) for copolymers with cholesterol and membrane phospholipid DPPG.

	φ_a (PEO block)	φ_b (DTR-XA or PPO block)	∂_T $(Jcm^{-3})^{1/2}$	χ Polymer/ cholesterol (298°K)
Cholesterol	-	-	17.75	-
Dipalmitoylphosphatidylglycerol (DPPG)	-	-	20.24	
PEO	1.0	0	21.99	2.73
PPO	0	1.0	17.78	0.0
PEO_{80}-PPO_{27}-PEO_{80} (P188)	0.817	0.183	21.22	1.83
PEO(5k)-$(DTE\text{-}SA)_{12}$-PEO(5k)	0.617	0.383	20.96	1.57
PEO(5k)-$(DTO\text{-}SA)_{10.5}$-PEO(5k)	0.617	0.383	20.89	1.50
PEO(5k)-$(DTD\text{-}DA)_{10.5}$-PEO(5k)	0.617	0.383	20.70	1.32
PEO(2k)-$(DTD\text{-}DA)_{10.5}$-PEO(2k)	0.392	0.608	19.93	0.722
PEO(5k)-$(DTE\text{-}SA)_{24}$-PEO(5k)	0.454	0.545	20.55	1.57
PEO(5k)-$(DTO\text{-}SA)_{27}$-PEO(5k)	0.358	0.642	20.14	0.868
PEO(5k)-$(DTD\text{-}SA)_{23}$-PEO(5k)	0.407	0.593	20.07	0.818
PEO(5k)-$(DTE\text{-}SA)_{24}$	0.294	0.706	20.08	0.825
PEO(5k)-$(DTO\text{-}SA)_{27}$	0.218	0.782	19.74	0.602
PEO(5k)-$(DTD\text{-}SA)_{23}$	0.255	0.745	19.58	0.509

It could therefore be predicted, based on compatibility increasing as $\chi \rightarrow 0$, that cholesterol would have the highest affinity for the most hydrophobic TyPS B-block, DTD-DA, and would also have high affinity for the PPO block of a triblock copolymer such as Poloxamer 188 (P188) comprised of PEO_{80} -PPO_{27} -PEO_{80}. However, the hydrophilic A-blocks of the TyPS and P188 significantly altered the anticipated affinity for cholesterol, as reflected in the relatively large Flory-Huggins parameter value for P188 (1.83) compared to those of the TyPS diblocks (0.509 to 0.82) and TyPS triblocks (0.722 to 1.57). It could also be predicted that the triblock TyPS comprised of PEO(5k)-$(DTO\text{-}SA)_{27}$-PEO(5k) and PEO(5k)-$(DTD\text{-}SA)_{23}$-PEO(5k), which were abbreviated as (T-DTO) and (T-DTD), would have the greatest binding affinity with the phospholipid DPPG and would therefore strongly insert into cell bilayer membranes comprised of DPPG and similar phospholipids.

The HLBs for prototype TyPSs, P188 and similar PEO-PPO-PPO triblocks, and cholesterol were calculated using the methods of Guo, et al, [6] and were summarized in Table 3:

Table 3. Calculated HLB values.

Composition	HLB
PEO(2k)-(DTE-SA)$_{12}$-PEO(2k)	60.8
PEO(5k)-(DTE-SA)$_{12}$-PEO(5k)	63.6
PEO(2k)-(DTO-SA)$_{10.5}$-PEO(2k)	28.9
PEO(5k)-(DTO-SA)$_{10.5}$-PEO(5k)	31.7
PEO(5k)-(DTD-SA)$_{10.5}$-PEO(5k)	12.4
PEO(5k)-(DTD-DA)$_{10.5}$-PEO(5k)	-7.50
PEO(5k)-(DTE-SA)$_{24}$-PEO(5k)	87.5
PEO(5k)-(DTO-SA)$_{27}$-PEO(5k)	19.3
PEO(5k)-(DTD-SA)$_{27}$-PEO(5k)	-19.9
PEO(5k)-(DTE-SA)$_{24}$	71.2
PEO(5k)-(DTO-SA)$_{27}$	2.90
PEO(5k)-(DTD-SA)$_{23}$	-36.2
(P188) PEO$_{80}$-PPO$_{27}$-PEO$_{80}$	28.7
(P85) PEO$_{26}$-PPO$_{40}$-PEO$_{26}$	24.3
(F88) PEO$_{103}$-PPO$_{39}$-PEO$_{103}$	25.8
(P105) PEO$_{37}$-PPO$_{56}$-PEO$_{37}$	17.3
(F127) PEO$_{100}$-PPO$_{65}$-PEO$_{100}$	17.7
Cholesterol	-2.93

As expected, as the degree of polymerization (dp) of the TyPS PEO A-blocks increased from 2kDa to 5kDa at constant B-block length, the copolymer HLB increased. (For the prototype TyPS with PEO(2kDa), the PEO dp = 2,000/44 = 45, and for TyPSs with PEO(5kDa), the dp = 5,000/44= 114.) And as the hydrophobicity of the TyPS B-block increased (i.e., as quantified in Table 1, DTD>DTO>DTE) the HLB decreased. The HLB calculated for P188 using the Guo, et al, equations was 28.7, which was in good agreement with the reported experimental value of 29; other published experimental HLB values for the Pluronics F88 (HLB=28), P105 (HLB=15) and F127 (HLB=22) were also in good agreement [7] but the experimental value for P85 (HLB=15) was not, perhaps due to a significant amount of diblocks which might be present in the commercial product.

1.2. Synthesis and structural characterization. An initial set of three diblock and three triblock TyPSs were synthesized using our established carbodiimide coupling reaction process. The tyrosine-derived monomers which comprised these TyPS were: DTE (desaminotyrosyl-tyrosine ethyl ester); DTO (desaminotyrosyl-tyrosine octyl ester); and, DTD (desaminotyrosyl-tyrosine dodecyl ester). The esters were made with suberic acid (SA) to form DTE-SA, DTO-SA and DTD-SA monomers, which were then polymerized using standard condensation reactions and end-capped at either one terminal end (to form the diblocks) or both terminal ends (to form the triblocks) with poly(ethylene glycol) methyl ether 5 kDa (mPEG(5k)) (Figure 3).

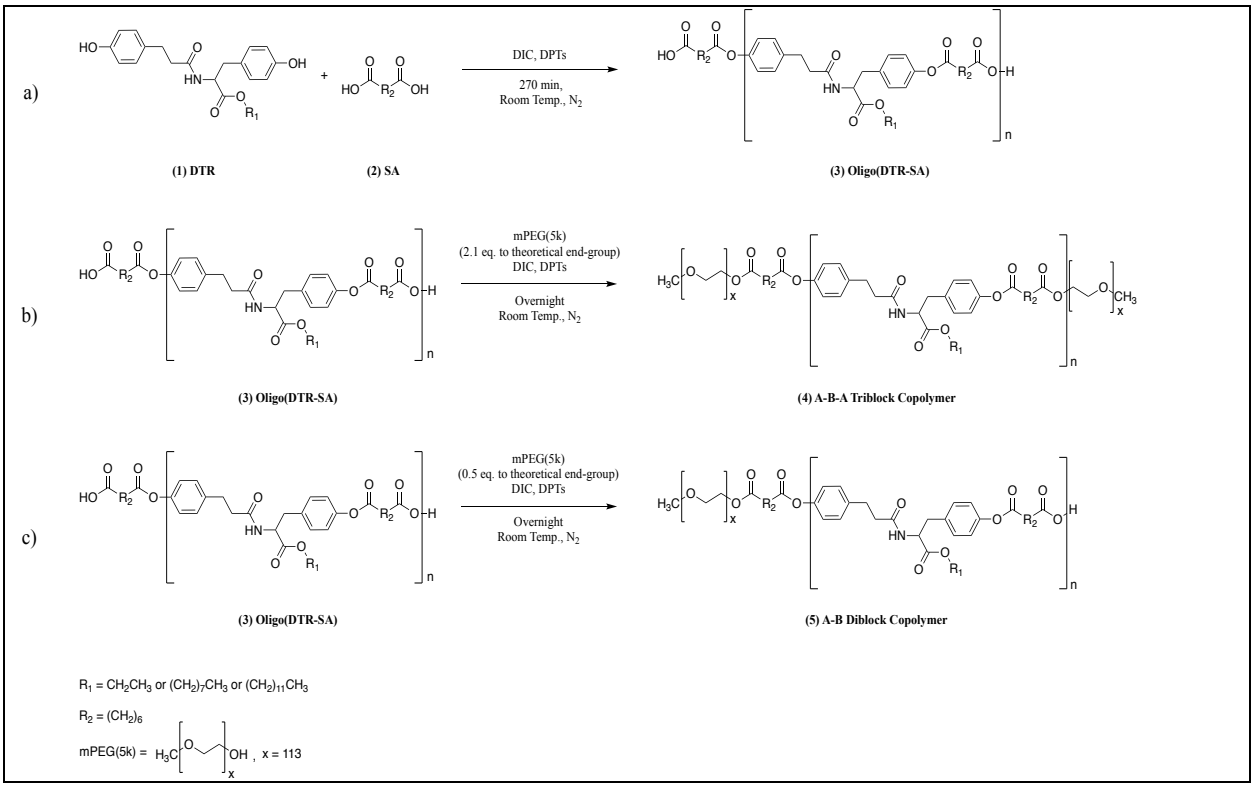

Figure 3. Synthesis scheme for diblock and triblock tyrosine-derived polymeric surfactants (TyPSs).

The DTR-SA blocks provided hydrophobic properties while the PEG blocks provided hydrophilic properties to these amphiphilic copolymers. Diblocks and triblocks with identical hydrophobic blocks were synthesized in order to compare their surfactant properties, including self-assembly into nanoparticles and their cholesterol encapsulation efficiencies. Prior research [20] had shown substantial systematic differences in those thermodynamic properties for diblock and triblock poly(alkylene oxide) polymeric surfactants based on analogous structures to the TyPS but comprised of poly(propylene oxide) (PPO) hydrophobic blocks with hydrophilic PEG (aka poly(ethylene oxide) (PEO)) blocks. Those differences were driven by the folding of the hydrophobic blocks in the triblocks, driven by molecular van der Waals forces and the relative physical size exclusion properties of the hydrophilic "head" groups and hydrophobic "tail" groups. Molecular mechanics studies previously performed by our group of TyPS structures was consistent with this picture of the folding of the hydrophobic DTR-SA blocks in aqueous solutions [8].

The molecular compositions of the synthesized TyPSs were confirmed by proton nuclear magnetic resonance (^{1}H-NMR) using a Varian VNMRS 500 MHz spectrophotometer and their molecular weights and molecular weight distributions were determined by gel permeation chromatography (GPC) using a mobile phase of tetrahydrofuran (THF)/butylated hydroxytoluene (BHT) and a refractive index detector (Table 4).

Table 4. TyPS molecular weight, polydispersity index (PDI) and degree of polymerization of tyrosine-derived hydrophobic (oligo(DTR-SA)) block.

Polymers	M_n (kDa)	M_w (kDa)	PDI	Oligo(DTR-SA) DP*
T-DTE	20.09 (0.05)	24.31 (0.03)	1.210 (0.001)	24
T-DTO	22.69 (0.01)	27.25 (0.05)	1.201 (0.002)	25
T-DTD	21.73 (0.06)	26.09 (0.06)	1.201 (0.001)	24
D-DTE	12.17 (0.02)	17.26 (0.01)	1.418 (0.003)	25
D-DTO	16.79 (0.03)	22.35 (0.03)	1.331 (0.001)	24
D-DTD	16.71 (0.05)	21.04 (0.04)	1.259 (0.003)	24

T: Triblock. D: Diblock. mPEG(5kDa) in all cases. M_n: number-average molecular weight. M_w: weight-average molecular weight. PDI: polydispersity index. DP: Degree of polymerization of the oligo(DTR-SA) block. Three separate batches of each TyPS were synthesized; the standard deviations of the independent triplicates are in parenthesis.

Task 2. Biophysical properties of TyPS.

2.1. Surface tension and critical aggregation concentration (CAC). The critical aggregation concentration (CAC) (aka critical micelle concentration, CMC) for each TyPS was determined by measuring the change in fluorescence of the dye Nile red in the bound (aggregate) state compared to the unbound state.[9] Surface tension measurements were not pursued due to the extremely low CAC values for the TyPS which could not be clearly determined by the traditional DuNouy tensiometer method. A range of 24 concentrations was used for each TyPS in phosphate buffered saline (PBS; pH7) from 9 x 10^{-2} µg/mL to 10 µg/mL. Fluorescence intensity scans were obtained at 25°C using a TECAN Spark multimode microplate reader with excitation wavelength set at 550nm and emission wavelength of 635 nm. The CAC was taken as the inflection point of data plotted as emission intensity versus log time. All of the diblock and triblock TyPS were found to self-assemble at very low concentrations (Table 5).

Table 5. Critical aggregation concentrations of TyPS in PBS at 25ºC. TyPS CACs were determined with Nile red probe at 25ºC; Pluronic CACs determined with pyrene probe at 37ºC[19]

TyPS	CAC (mM)
T-DTE: PEO(5k)-(DTE-SA)$_{24}$-PEO(5k)	0.027
T-DTO: PEO(5k)-(DTO-SA)$_{27}$-PEO(5k)	0.028
T-DTD: PEO(5k)-(DTD-SA)$_{23}$-PEO(5k)	0.020
D-DTE: PEO(5k)-(DTE-SA)$_{24}$	0.063
D-DTO: PEO(5k)-(DTO-SA)$_{27}$	0.017
D-DTD: PEO(5k)-(DTD-SA)$_{23}$	0.030
(P188;F68): PEO_{80}-PPO_{27}-PEO_{80}	0.48
(P85): PEO_{26}-PPO_{40}-PEO_{26}	0.065
(F88): PEO_{103}-PPO_{39}-PEO_{103}	0.25
(P105): PEO_{37}-PPO_{56}-PEO_{37}	0.001
(F127): PEO_{100}-PPO_{65}-PEO_{100}	0.006

No strong systematic relationship between the TyPS compositions and their experimental CACs was observed. The value obtained here for the T-DTO was in reasonably good agreement with

experimental values which our group previously obtained for similar TyPS with different B-block degrees of polymerization: CAC= 0.26 µg/mL using static light scattering [1] and 2.2 µg/mL using pyrene fluorescence measurements.[8] It is noted that CAC values for the Pluronics have been obtained by several different research groups using diverse methods (fluorescent probe binding and light scattering) and there is poor agreement between those published values.[7] For the Pluronics (Poloxamers), it has been shown that the CAC values are inversely proportional to the temperature and there is no reported CAC for P188 at 25°C. In contrast, the TyPS all self-assemble at 25°C with very low CACs.(Table 5).

In contrast to the TyPS, the CAC for P188 has been found to be orders of magnitude greater; i.e., P188 is far less surface active than the TyPSs. Our group previously found using pyrene fluorescence that the CAC for P188 is 0.44mg/mL at 37°C [8] and an even higher CAC of 4.0mg/mL obtained by similar pyrene fluorescence at 37°C has been reported.[22] The P188 CAC determined by Langmuir trough surface pressure was reported to be 0.125mM (1.0 mg/mL) at 30°C.[23] Although these P188 CACs reflect commonly observed experimental variations, it was clear that the TyPS self-assembled at far lower concentrations than P188. That observation was consistent with thermodynamic theory [10] which predicted that the CACs would be directly related to the copolymer solubility parameters as can been seen from the calculated ∂_T values in Table 2.

2.2. Langmuir film balance (LFB) measurement of surface pressure – mean molecular area (π–A) isotherms. Poloxamer 188 has been shown to insert into phospholipid monolayer films at low surface pressures and to diffuse out of the films at high surface pressures.[11] That behavior, which was correlated with the therapeutic effects of P188 on repair of injured muscle and nerve tissue [12], provided the initial impetus for this research project.

The effect of TyPSs on the surface pressure of phospholipid monolayers was determined using a double barrier Langmuir film balance (KSV Minimicro surface balance with an 8400mm^2 single trough, KSV Instruments, Finland) equipped with a microroughened platinum Wilhemy plate (Biolin Scientific/Nanoscience Instrument, USA) and KSV LayerBuilder control software (v.3.3). Filtered phosphate buffer solution (MP Biomedicals, USA) was used as the aqueous subphase at ambient temperature. Phospholipid monolayers were prepared from chloroform solutions of the following three membrane phospholipids:1)1,2-Dipalmitoyl-sn-glycero-3-phospho-rac-(1-glycerol) (DPPG); 2) 1,2-Dipalmitoyl-sn-glycero-3-phosphocholine (DPPC); and, 3) 1,2-Dipalmitoyl-rac-glycero-3-phospho-L-serine,~98% (DPPS) (Sigma-Aldrich, USA). The chloroform solutions at 0.2mg/ml concentration were deposited on the film balance aqueous surface using a glass micro syringe (Hamilton, USA) at a constant volume of 15 microliters to create the phospholipid monolayers. Aqueous TyPS suspension was injected into the film balance subphase using a side port to prevent physical disturbance of the phospholipid monolayer. The compression barrier speed was kept constant at 20 cm^2/m. Three or more isotherms were collected per each injection. Note that the TyPS concentrations in the aqueous subphase were below their measured CACs.

The interaction of the polymeric surfactants with the phospholipid monolayer films measured using a Langmuir film balance can in theory be quantified by measuring the areas under the curves (AUCs) of the surface pressure (π) versus mean molecular area (A) to obtain the excess Gibbs free energy of mixing, ΔG_{exc} ,

$$\Delta G_{exc} = \int [A_{1,2} - (x_1 A_1 + x_2 A_2)]\, d\pi \qquad \text{(Equ. 1)}$$

where: $A_{1,2}$ = mean molecular area in the mixed monolayer films at surface pressure π; A_1 and A_2 = molecular areas in the neat phospholipid monolayer and neat polymeric surfactant,

respectively, at a given π; and, x_1 and x_2 = mole fractions of the components 1 and 2 in the mixed monolayers.[13,14]

The molecular weights of the three phospholipids, DPPC, DPPS and DPPG, were 734, 736 and 745 g/mole, respectively. Monolayer films were prepared by applying 15μL of 0.2mg/mL stock solutions of the phospholipids dropwise onto the aqueous surface in the film balance trough. The mole fractions of the phospholipid, X_1, and polymeric surfactant, X_2, were calculated, as illustrated here for DPPS with 0.25mL of 33mg/mL T-DTD injected into the aqueous subphase of the Langmuir film balance trough:

- n_1 = 15μL x 0.2mg/mL x 1mole/736g DPPS = 4.09 x10^{-9} mole DPPS;
- n_2 = 0.25mL x 33mg T-DTD/mL x 1mole/(21.7 x 10^3 g) = 3.80 x 10^{-7}mole T-DTD;
- $X_1 = n_1/(n_1 + n_2)$ = 4.09 x10^{-9}/ (4.09 x10^{-9} + 3.80 x 10^{-7}) = 0.01; X_2 = 0.99.

That is, the mole fraction of phospholipid in each film was almost negligible compared to that of the TyPS, assuming that all of the TyPS was present in the monolayer film. Given that the critical aggregation concentrations (CACs) for the TyPS were in most cases all greater than or equal to the TyPS concentrations used, it is reasonable to assume that some, but not all, of the TyPS was present in the surface film. Consequently, the contributions of the phospholipids alone to the excess free energy of mixing, as given by the second term in equation (1), would be expected to be small compared to that of the TyPS, which is given by the third term in equations (1). However, experiments were not run to obtain that third term (i.e., the surface pressures of TyPS solutions in the absence of the phospholipid were not measured). For this reason, it was not possible to calculate the excess free energy of mixing in the surface films and only qualitative differences could be distinguished for the mixed films.

Comparison of the triblock and diblock TyPS in DPPG. With the exception of the diblock DDTE, at approximately 15μM concentration all of the TyPS shifted the curves toward lower molecular area than the neat DPPG at a given surface pressure, which was indicative of the mixtures being thermodynamically more stable than the neat DPPG film; i.e., the excess free energies of mixing are all negative (Figure 4). The differences between the three triblock TyPS are relatively small compared to those of the diblocks. The DDTD and TDTD are quite similar in behavior. There was no strong correlation with triblock TyPS HLBs or solubility parameters whereas the diblocks increased packing density (decreased molecular area) as their HLBs decreased (i.e., the more hydrophobic, the greater the packing).

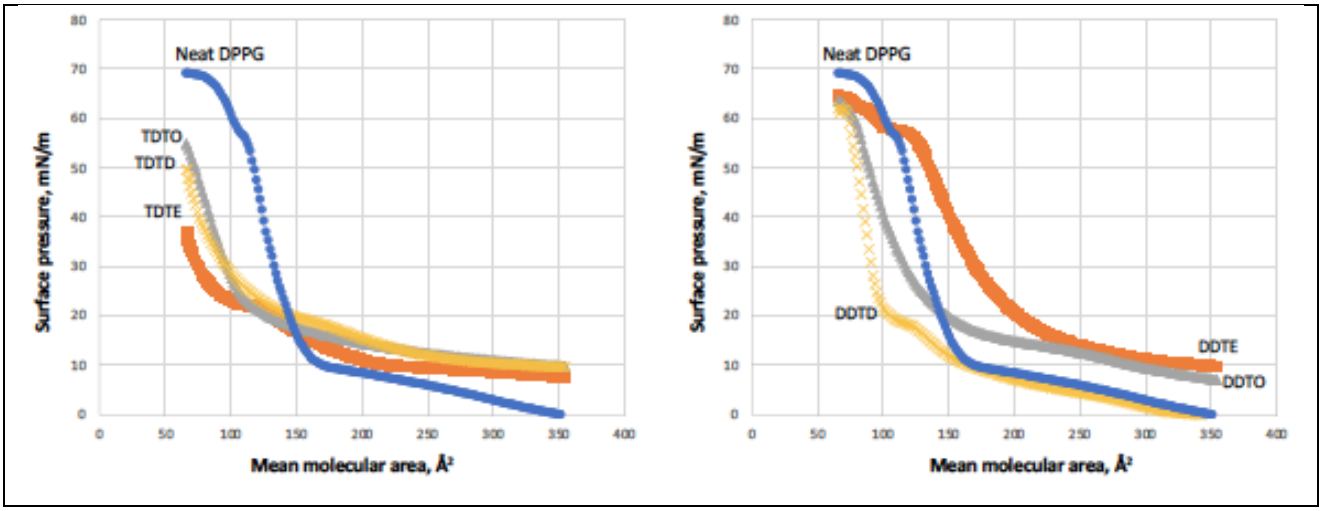

Figure 4. DPPG monolayer film interactions with triblock (left) and diblock (right) TyPS.

Comparison of the triblock and diblock TyPS in DPPS. In mixed DPPS films at approximately 13μM TyPS concentration, the triblocks increased the surface pressure at any given molecular area compared to the diblocks and the neat DPPS film (Figure 5). TDTD and TDTO produced phase transitions from LE to I at 22mN/m and 18 mN/m, respectively, with the TDTD producing a more pronounced transition. The diblocks also increased the surface pressures at any given molecular area compared to the neat DPPS film and the DDTD produced a phase shift from LE to I at 18mN/m.

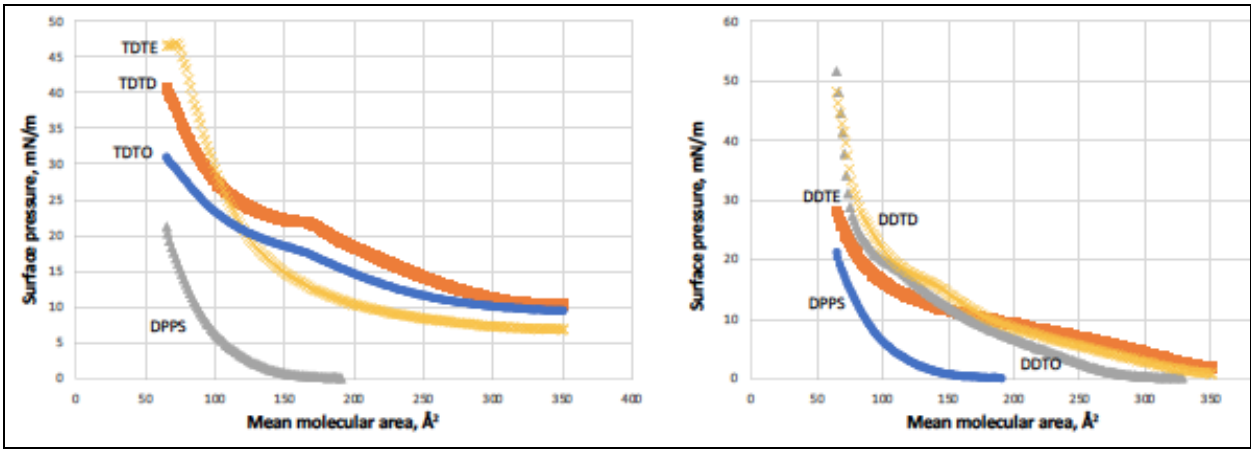

Figure 5. DPPS monolayer film interactions with triblock (left) and diblock (right) TyPS.

Comparison of the triblock and diblock TyPS in DPPC. The diblocks were compared here at 25-35μM while the triblocks were compared at 7μM due to the limited available experimental data (Figure 6). The triblock TDTD caused a pronounced LE-I phase transition at 22mN/m, TDTO caused only a slight Le-I transition and TDTE did not cause a phase transition. Similar but less pronounced phase transitions were observed for the DDTO and DDTD. At a given surface pressure, e.g., 20mN/m or 35mN/m, the molecular areas decreased with increasing hydrophobicity of the diblocks, while the opposite trend was observed with the triblocks (i.e., at a given surface pressure, the molecular areas increased with increasing hydrophobicity of the triblocks).

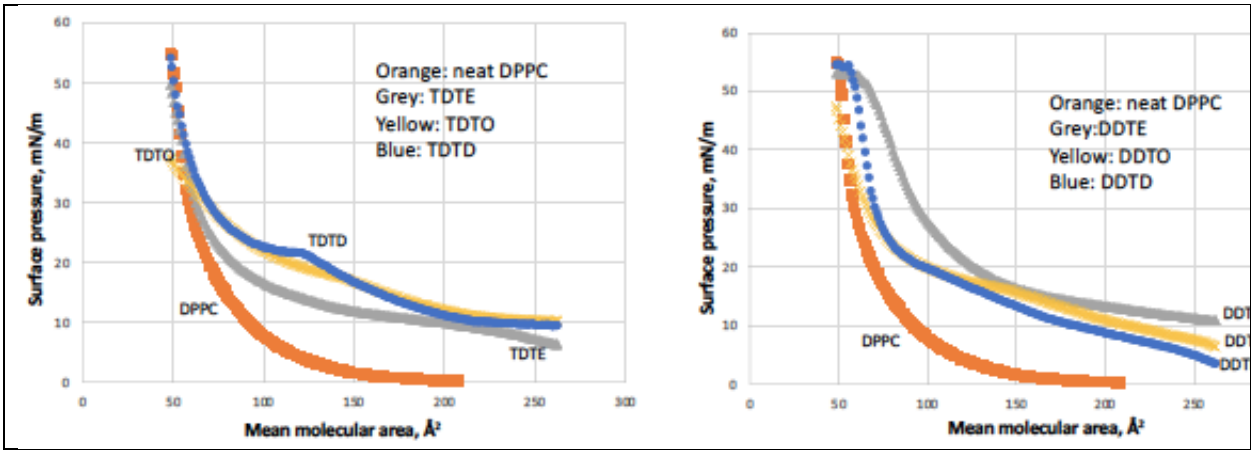

Figure 6. DPPC monolayer film interactions with triblock (left) and diblock (right) TyPS.

Comparison of T-DTD effects on Langmuir monolayer films of DPPC, DPPS and DPPG.
The chemical structure of the phospholipid affected the interaction with the most hydrophobic TyPS, T-DTD (Figure 7). At approximately the same molar T-DTD concentration (13-15μM), the molecular packing of the mixed DPPG film was much greater (much closer together) than the DPPS film, which in turn was only slightly greater than the DPPC film at any given surface pressure. T-DTD caused an LE-I phase transition in all three phospholipids at the same 22mN/m surface pressure.

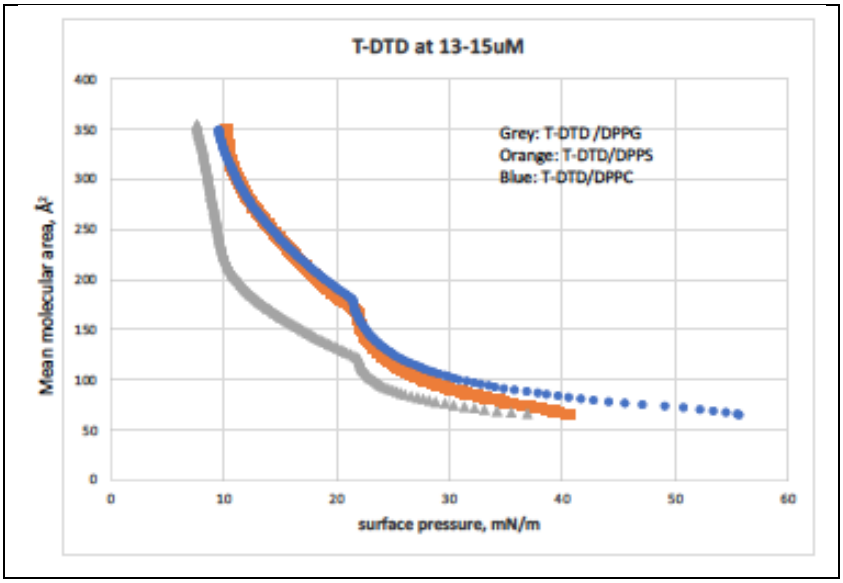

Figure 7. Effect of phospholipid composition on interactions with triblock TyPS, T-DTD, in Langmuir monolayer films.

Comparison of the interaction of DPPC Langmuir monolayer films with P188, T-DTD and T-DTD/5%Cholesterol.
In DPPC mixed films, P188 data at concentrations of 0.28mg/mL and 0.56mg/mL were essentially identical and were similar to that of T-DTD, although T-DTD produced a phase transition at approximately 22mN/m whereas P188 did not. At surface pressures above 35mN/m, P188 data were equivalent to that of the neat DPPC, which again supports the conclusion of Maskarinec, et al,[11] that the polymer is squeezed out of the monolayer film at high surface pressures. At lower surface pressures, P188, T-DTD and the FNP of T-DTD/Cholesterol all increased the molecular surface area compared to neat DPPC, indicative of disrupting the packing of the DPPC chains. Note that the FNP, TDTD/5%cholesterol, appeared to cause two distinct phase transitions, one at 22mN/m and another at 31mN/m, whereas T-DTD caused only a single LE-I transition at 22mN/m.

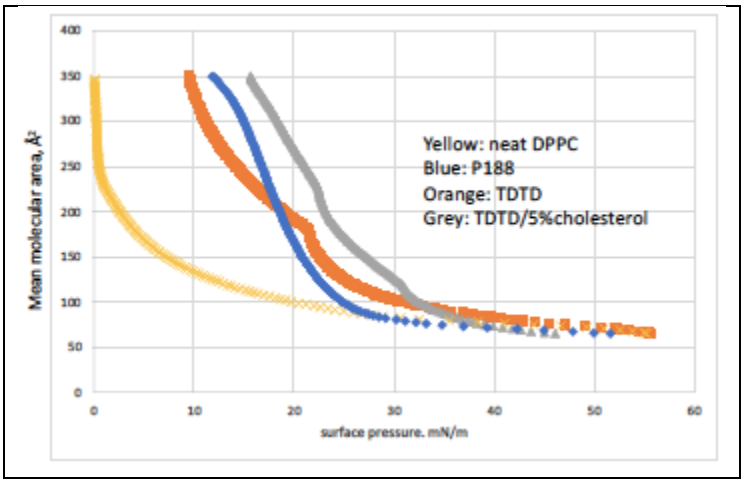

Figure 8. Interaction of P188 and TyPS with DPPC monolayer films.

A key conclusion from this comparison of TDTD and P188 was that these triblock copolymers have quantitatively comparable effects on the DPPC film, although the molar concentration of P188 (33μM) needed was far greater than the TDTD (15 μM).

Mixed Langmuir monolayer films of DPPC and PEG 3.5kDa. As seen in Figure 9 on the left, the behavior of PEG in mixed films with DPPC was different than that of P188 and the TyPS copolymers; above 10mN/m surface pressure, PEG reduced the molecular area compared to the neat DPPC. The areas under the curves (AUCs) were less for PEG than neat DPPC or the mixed films with P188 and the TyPSs (Figure 8), which was indicative of a decrease in the excess free energy of mixing. There was a very slight dependence of PEGs behavior on the PEG concentration, with the highest concentration causing the greatest increase in packing of the mixed DPPC film; e.g., at 35mN/m, the molecular surface areas decreased from 72 Å^2 for neat to DPPC to 59 Å^2, 53 Å^2 and 50 Å^2 at PEG = 0.28mg/mL, 0.56mg/mL and 0.72mg/mL, respectively. The almost vertical and linear behavior below 10mN/m was consistent with a published study [15] in which the surface pressure of neat PEG in aqueous solutions approached upper asymptotic limits of between 6mN/m and 10mN/m as a function of increasing PEG concentration and increasing PEG molecular weight. There was a linear dependence of the AUC on PEO concentration, as shown in the Figure 9 on the right, which was indicative of increasing stability of the mixed PEO-DPPC films with increasing PEO concentration.

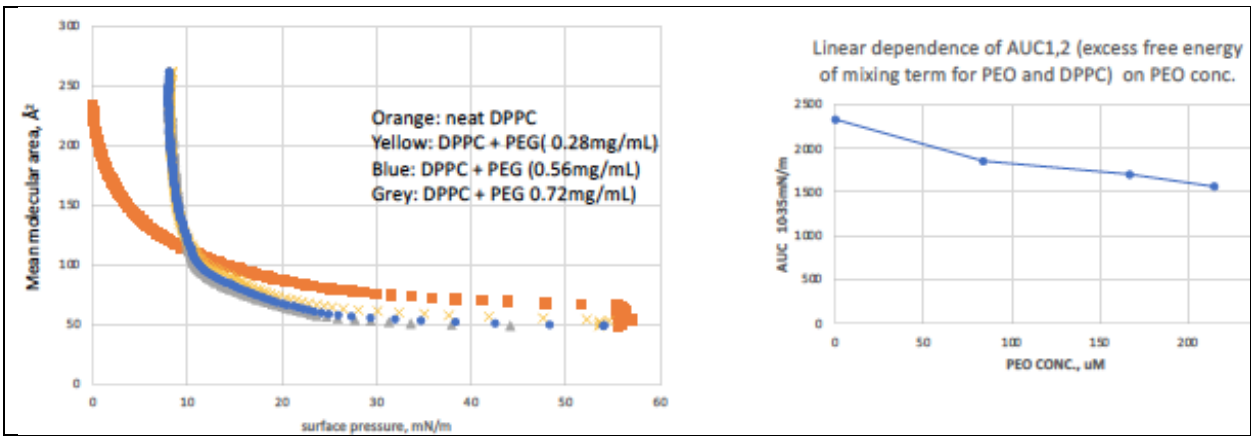

Figure 9. PEG effects on DPPC monolayer films.

Mixed monolayers of DPPC with T-DTD and with functional nanospheres (FNPs) of T-DTD/5%Cholesterol. At surface pressures below 35mN/m, the T-DTD/5%cholesterol nanospheres produced higher molecular areas than T-DTD, indicative of cholesterol insertion causing a further disordering of the DPPC film (Figure 10). Another way to look at this was that the surface tension with T-DTD/cholesterol was much lower than with T-DTD alone, demonstrating that cholesterol had been delivered into the surface film and disrupted the packing of the DPPC chains. Above 35mN/m, the molecular areas were essentially the same, indicating that the T-DTD and cholesterol were squeezed out of the monolayer films. The T-DTD concentration in these runs was 0.33mg/mL (15 μM) for both T-DTD alone and in the T-DTD/cholesterol nanosphere formulation.

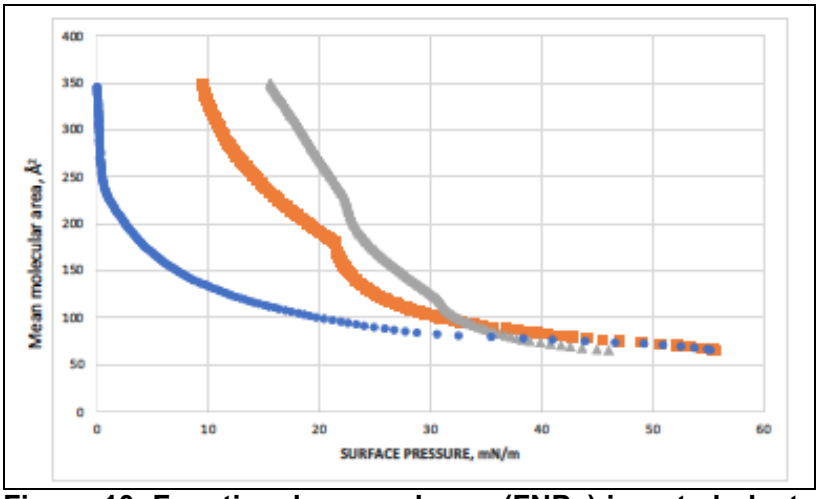

Figure 10. Functional nanospheres (FNPs) insert cholesterol into DPPC monolayer films. Blue: neat DPPPC (control). Orange: DPPC with T-DTD. Grey: DPPC with FNP of T-DTD/ 5%cholesterol.

Task 3. Biophysical properties of Fusogen Nanoparticles (FNPs)

The purpose of preparing nanoparticles loaded with cholesterol was to determine if they would provide controlled delivery of cholesterol to increase its concentration levels in axonal membranes. Cholesterol was known to be a major natural component of eukaryotic cell membranes and acted as a fusogen to modulate membrane fluidity and permeability.[16]

3.1. Fusogen Nanoparticles of tyrosine-derived polymeric surfactants (TyPS) and cholesterol. Nanospheres of unloaded TyPS and TyPS loaded with cholesterol were prepared using our previously developed nanoprecipitation process.[2] The particle sizes of the resultant FNPs were determined using the Malvern Zetasizer. The hydrodynamic particle properties of the unloaded TyPS nanospheres were summarized in Table 6:

Table 6. Unloaded TyPS nanospheres particle size distributions

Copolymer	Z-Average Size (nm) (n=3)	Average PDI (n=3)	Peak Size (d.nm) (n=3)	St. Dev - Peak Distribution (d.nm) (n=3)

T - PEG(5k)/DTE-SA	35.5 (0.6)	0.269 (0.021)	34.4 (0.2)/2659 (1209)	10.3 (0.2)/970 (83)
T - PEG(5k)/DTO-SA	33.4 (0.2)	0.056 (0.004)	35.7 (0.1)	9.5 (0.1)
T - PEG(5k)/DTD-SA	33.7 (0.2)	0.061 (0.007)	36.3 (0.1)	9.7 (0.1)
D - PEG(5k)/DTE-SA	188.9 (8.9)	0.222 (0.024)	245.6 (22.9)	134.7 (30.7)
D - PEG(5k)/DTO-SA	143.5 (3.4)	0.126 (0.009)	165.7 (2.8)	63.7 (3.3)
D - PEG(5k)/DTD-SA	174.8 (0.7)	0.136 (0.007)	204.6 (0.6)	79.0 (3.7)

In parenthesis is the standard deviation of the triplicate. All samples met the DLS quality criteria for analysis. T – Triblock, D – Diblock.

The particle sizes of the cholesterol-loaded FNPs were summarized in Table 7. Most of the particle size distributions were bimodal, which was indicative of small populations of unloaded nanoparticles and cholesterol-loading nanoparticles. Nevertheless, the average particle sizes were all small enough to be suitable for intravenous injections and other common drug delivery methods.

Table 7. TyPS-cholesterol FNP hydrodynamic particle diameters

	FNP hydrodynamic diameter (nm) (Z-average) at targeted load levels				
	1%	**3%**	**5%**	**7%**	**10%**
T-DTE-PEG5k	44	42	47	45	43
T-DTO-PEG5k	34	72	95	118	116
T-DTD-PEG5k	34	35	35	48	114
D-DTE-PEG5k	220	203	230	222	207
D-DTO-PEG5k	139	137	99	98	99
D-DTD-PEG5k	171	175	175	183	175

The cholesterol loading levels of the FNPs were summarized in Figure 11:

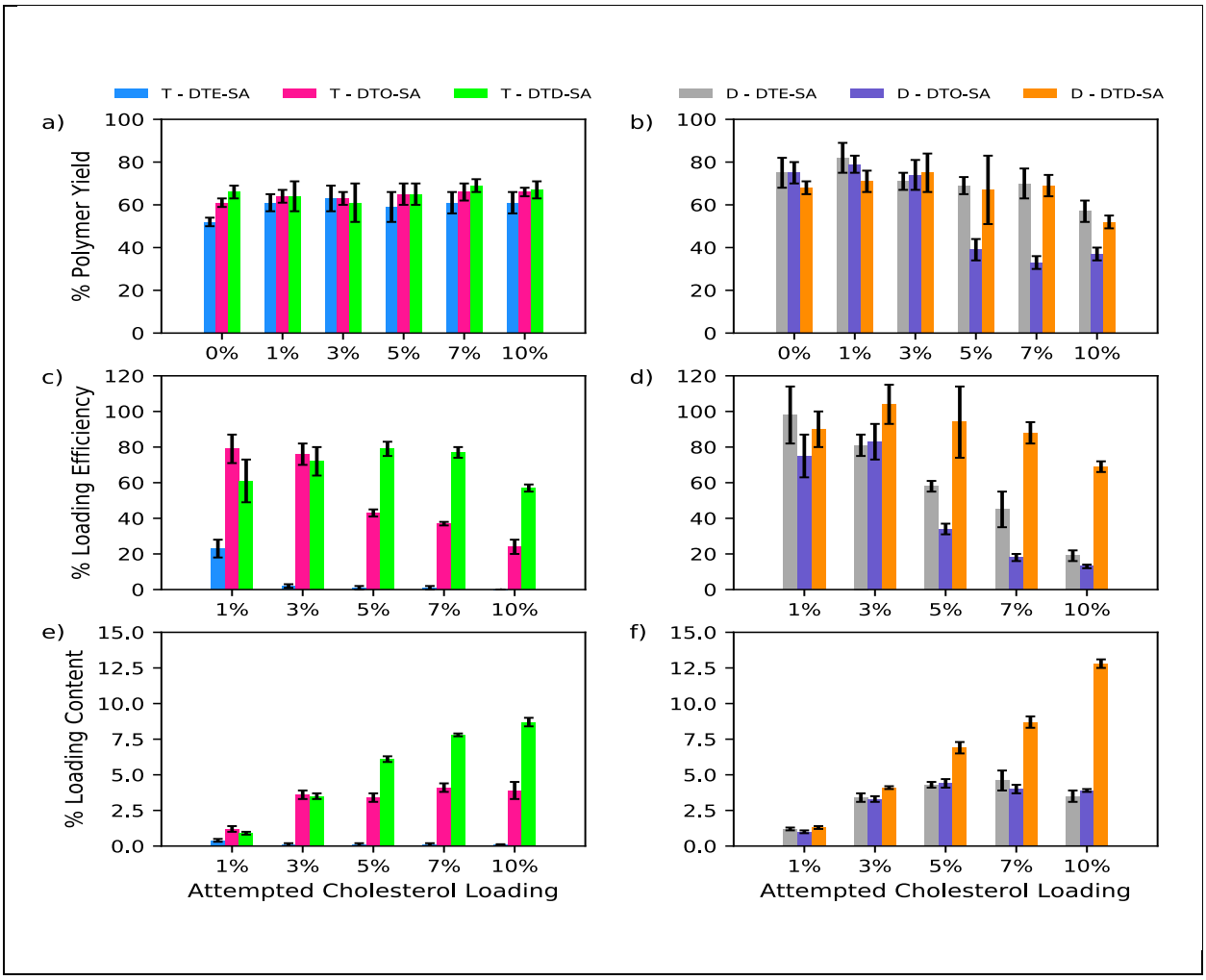

Figure 11. TyPS-cholesterol FNP yield, loading efficiency and loading level. a) % polymer yield of triblock copolymers, b) % polymer yield of diblock copolymers, c) % loading efficiency of triblock copolymers, d) % loading efficiency of diblock copolymers, e) % loading content of triblock copolymers, f) % loading content of diblock copolymers. Triblock copolymers: PEG(5k)/DTE-SA in blue, PEG(5k)/DTO-SA in pink, PEG(5k)/DTD-SA in green. Diblock copolymers: PEG(5k)/DTE-SA in grey, PEG(5k)/DTO-SA in purple, PEG(5k)/DTD-SA in orange.

The FNPs prepared with the diblock D-PEG(5k)/DTD-SA and triblock T-PEG(5k)/DTD-SA were the most effective for attaining high cholesterol loading levels. That result was consistent with the Flory-Huggins interaction parameter values (Table 2).

3.2. Cholesterol controlled release kinetics from the FNPs. Despite the extremely low solubility of cholesterol in aqueous solution, 9.5 x 10^{-5} mg/mL, a linear calibration curve was obtained using high performance liquid chromatography (HPLC) and the release of cholesterol from the functional nanoparticle (FNP) comprised of triblock TyPS T-DTD and 5% cholesterol (Figure 12) was obtained by equilibrium membrane dialysis in PBS. Although there was significant variation in individual time points, the release appeared typical of FNP release of other hydrophobic drugs with a rapid early stage followed by a slower stage.

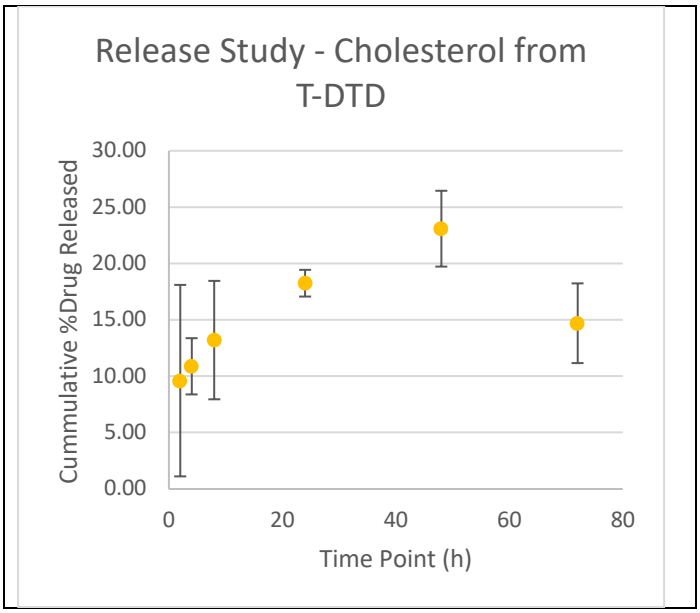

Figure 12. Controlled release of cholesterol from an FNP of T-DTD/5%cholesterol

3.3. Partition coefficients, $log_{10}P(o/w)$ for the FNPs. No data have been obtained related to this Task due to disruptions caused by the COVID-19 pandemic and the closure of the Kohn Lab at Rutgers.

Task 4. IACUC and ACURO animal protocol reviews

4.1. Document rat tibial nerve protocol and submit to Rutgers IACUC and US Army ACURO. The rat nerve injury protocol for evaluation of the in vivo fusogenic efficacy of TyPS-cholesterol FNPs was reviewed and approved in 2020 by the Rutgers Institutional Animal Care and Use Committee (IACUC) and the US Army Animal Use and Care Review Office (ACURO). The protocol was subsequently revised and approved by the Rutgers IACUC and then by the ACURO on 2 June, 2021. Briefly, in the protocol the rat tibial nerve will be isolated, surgically transected, immediately repaired with microsutures to reproduce the axonal overlapping routinely achieved in standard end-to-end nerve coaptation in clinical practice, treated with the fusogens and characterized using electrophysiological and histological measurements.

Specific Aim 2: Evaluation of functional nanoparticle (FNP) *in vitro* axonal membrane repair and cytotoxicity

Task 5: FNP repair of dorsal root ganglion (DRG) axon membranes.

5.1: Compare the efficacy of FNPs, PEG and P188 for fusion of severed DRG axon fusion based on fluorochrome dynamics.

Subtask 5.1 was 30% completed at the end of year 1 (2020) and has been 100% completed in year 2 (2021).
In this in vitro study, the aim is to demonstrate axonal fusion using rat dorsal root ganglions (DRGs). In the past two years, we developed: 1) a novel 3d scaffold design and fabrication; 2) in vitro culture of rat embryo DRGs to obtain significant growth of axons; 3) a practical and

reproducible technique for a mechanical blade-cut of single axons; 4) a low-cost technique to differentially stain the DRGs with red and green vital fluorochromes markers with did not affect cell viability; 5) completed testing of five groups using the in vitro DRG model.

Table 8 Five experiment groups and replicates in DRG axon fusion experiment

Group	Description	Replicates
1	Control (no fusogen)	3
2	PEG with PBS	6
3	Poloxamer	4
4	PBS with unloaded Tyrospheres	3
5	PBS with Cholesterol-loaded Tyrospheres	5

Overall, there has been 24 axonal fusion DRG experiments in the two years. All five groups of interest had at least 3 replicates. Groups outside interest were introduced in experiments aimed at refining the protocol. In all experiments, phase contrast images and live-fluorescence images were taken before and after administration of fusogen preparations (after 5 and 10 minutes; shorter and longer intervals have been occasionally integrated).

Results

End-to-end vertebrate axonal fusion was never observed in any preparation. This confirms the preliminary findings in the year 1 report. Our results have shown that the blade-cut of a single axon has nearly always produced a gap where axons have no tendency to spontaneous fusion. Distal axonal stumps have gradually lost fluorescence and have shown the tendency to retract from the cutting line; they degenerate in granules in about 48 hours. Please see the year 1 report. At higher magnification, images obtained from the Helium-Ion microscope suggest that a possible side-by-side fusion of some length of these axons has occurred. It is also possible that areas enlarge as a consequence of axons being pulled by a side-by-side fusion.

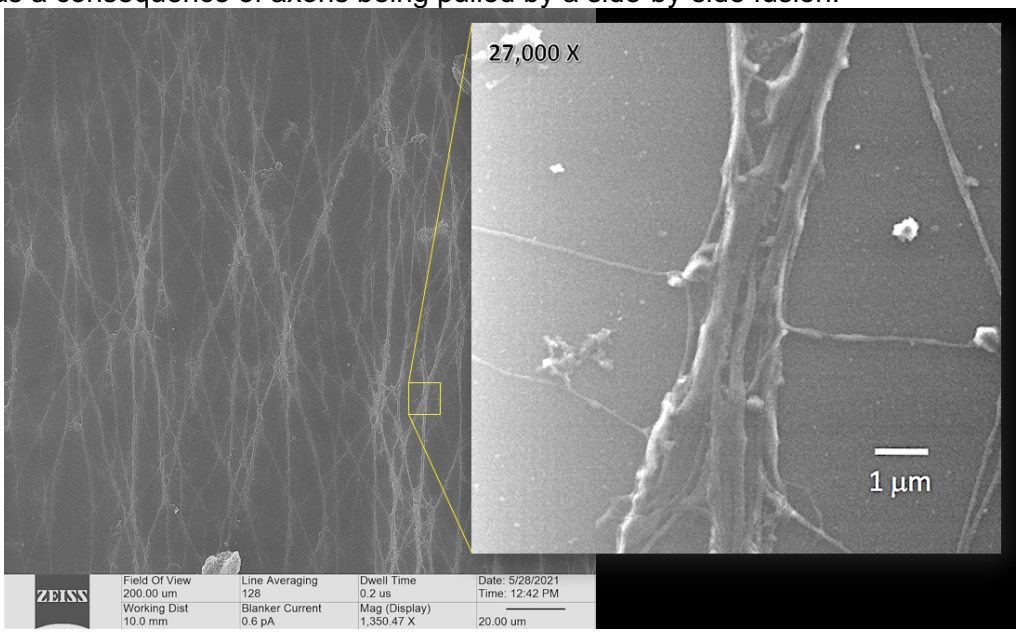

Figure 13: Helium-ion microscopy shows axons entanglement. The high-resolution image showed entangled axons possibly fused together after PEG administration. Axons appear to be pushed against each other and bent from their original path.

Discussion
An "end-to-end" axonal fusion will be difficult to achieve due to the magnitude of difference between the dimensions of the single axons and that of the gap in the DRG model. A "side-by-side" fusion is a possibility, but it is difficult to quantify fusion using Helium-Ion microscopy. We have decided to move forward with the in vivo animal study.

5.2: Determine the efficacy of Fusogen Nanoparticles (FNPs) for delivery of cholesterol to DRG axonal membranes based on quantitative HPLC analysis. No work has been performed on this Task.

Task 6. Cytotoxicity of Fusogen Nanoparticles (FNPs).

6.1. Determine the cytotoxicity of FNPs, TyPSs, PEG and P188 based on viability assays for human endothelial cells and primary nerve cells.
The viability of human dermal microvascular endothelial cells (HDMECs) in the presence of TyPS was normalized to that of untreated HDMECs and, as shown in Figure 14, the HDMECs maintained between 100% and 80% viability even at the high dosage of 10% TyPS solutions. Based on the criteria in ISO Standard 10993-5, it was concluded that none of the TyPS were cytotoxic to HDMEC. That result was consistent with our previous studies with similar TyPS compositions.

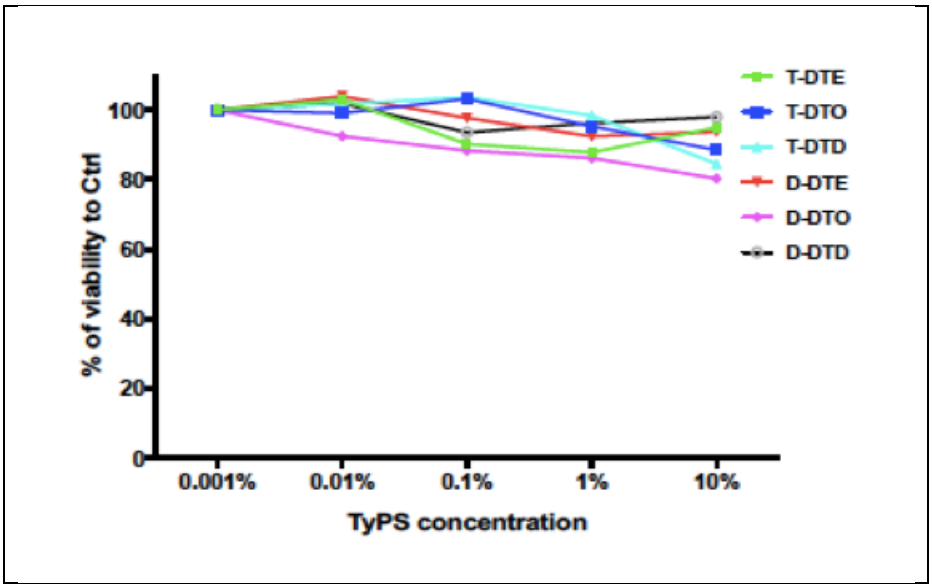

Figure 14. Viability of human dermal microvascular cells in the presence of increasing concentrations of diblock and triblock TyPS. PEG(5kDa) used in all of these TyPS.

The viability of the HDMECs was increased by the diblock and triblock FNPs and at the highest tested concentration of 10% FNP, the triblocks were particularly effective at increasing the cell viability whereas PEG actually demonstrated some cytotoxicity at that high 10% concentration (i.e., at a lower concentration than the 50% which was typically used in PEG cell fusion applications) (Figure 15).

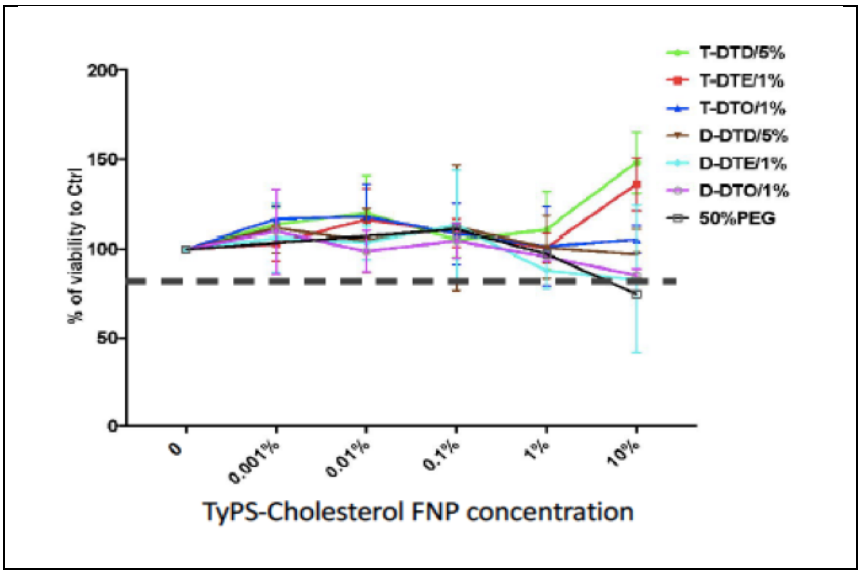

Figure 15. Viability increase of HDMECs by TyPS-cholesterol FNPs. Cholesterol binding levels (%) are given in the insert for each TyPS. FNPs with binding levels of 5% did not produce stable dispersions except with the most hydrophobic (lowest HLB) TyPS, T-DTD and D-DTD.

Neuronal cell viability and fusion were determined by flow cytometry with B35 rat neuroblastoma cells treated with PEG, P188 and the diblock and triblock TyPSs. Flow cytometry was not specifically included in the original project plan but was considered to offer potentially important insights into the cytotoxicity and fusogenic activity of the fusogens which cannot be as readily determined by other methods. It remains to be seen if the cell membrane processes observed with flow cytometry in this neural cell line are conserved in axonal fusion. This flow cytometry work was not carried out nor paid for by the Fusogen Nanomedicine project. Rather, it was another project at Rutgers conducted under a separate NIH T-32 fellowship project which had relevant information for this project and the results are cited here. The method used here followed a published approach which had been used to demonstrate the fusion of rat B35 neuroblastoma cells by 50% PEG solution.[17]

The flow cytometry experiments were repeated in triplicates and analysis of variance (ANOVA) for each time point was performed. The results of the flow cytometry experiments were summarized in Table 9. At 1 min exposure time, PEG was found to be superior to the diblock TyPS while the triblock TyPS and P188 were relatively ineffective. However, the cytotoxicity of PEG precluded measurements at 2hr or 24hr exposure times, whereas the TyPS and P188 appeared to produce fusion and maintain viability at those longer exposure times.

Table 9. Flow cytometry of neuroblastoma cells treated with PEG, P188, TyPSs and FNPs

Treatment	Dosage (mg/mL)	Exposure Time	Whole Cell Viability (%)	Fused Cells (%)
PBS	-	1 min	81.8+/-18.7	5.5 +/-1.2
PBS	-	2 hr	49.0+/-8.8	0.65+/-0.07
PBS	-	24 hr	27.7+/-9.5	8.3+/-1.4
PEG	500	1 min	79.8+/-4.2	11.3+/-1.0
PEG	500	2 hr	0	0
PEG	500	24 hr	-	-

P188	40	1 min	81.3+/-0.4	4.7+/-0.5
P188	40	2 hr	75.2+/-0.6	4.0+/-0.2
P188	40	24 hr	18.6+/-3.4	11.9+/-1.4
T-DTD	40	1 min	90.4+/-5.8	2.9+/-0.6
T-DTD	40	2 hr	76.2+/-1.7	4.1+/-0.2
T-DTD	40	24 hr	49.2+/-2.8	7.6+/-0.8
FNP T-DTD/Cholesterol 5%	40	1min	63.3+/-3.8	3.4+/-0.2
FNP T-DTD/Cholesterol 5%	40	2 hr	77.7+/-1.9	4.3+/-0.3
T-DTO	40	1 min	83.1+/-4.6	2.7+/-0.4
T-DTO	40	2 hr	72.3+/-2.9	2.3+/-0.3
T-DTO	40	24 hr	50.6+/-5.4	7.9+/-0.4
FNP T-DTO/Cholesterol 1%	40	1min	47.1+/-23.3	2.6+/-2.2
FNP T-DTO/Cholesterol 1%	40	2 hr	75.9+/-3.3	3.8+/-0.4
T-DTE	40	1 min	83.2+/-2.9	1.9+/-0.1
T-DTE	40	2 hr	75.6+/-0.6	2.7+/-0.1
T-DTE	40	24 hr	49.0+/-6.8	8.2+/-0.6
FNP T-TDE/Cholesterol 1%	40	1min	62.0+/-2.6	4.6+/-0.2
FNP T-TDE/Cholesterol 1%	40	2 hr	78.6+/-0.8	3.0+/-0.2
D-DTD	40	1 min	65.1+/-4.0	6.7+/-0.6
D-DTD	40	2 hr	tbd	tbd
D-DTD	40	24 hr	14.0+/-0.8	5.8+/-0.9
D-DTO	40	1 min	67.2+/-2.6	6.7+/-0.5
D-DTO	40	2 hr	tbd	tbd
D-DTO	40	24 hr	12.7+/-2.7	6.4+/-1.2
D-DTE	40	1 min	38.0+/-5.8	4.8+/-0.5
D-DTE	40	2 hr	tbd	tbd
D-DTE	40	24 hr	20.8+/-2.3	6.4+/-0.5

Compare the efficacy of FNPs, PEG, and P188 for fusion on L929 cells

In year 3, we introduced another cell culture system for screening the fusogenic activity. L929 is an established mouse fibroblast cell line used to study cell fusion by PEG. We tested triblock and deblock for one-hour treatment time with various concentrations and post-treatment periods. We have not observed any significant cell fusion from these fusogens when compared with controls. PEG, on the other hand, produced significant cell fusion on L929 cells with one minute incubation time. When PEG was combined with P188, we observed a significantly higher fusion index (Figure 16). This effect was not due to P188 because P188 alone did not promote cell fusion on L929 cells. This result indicated that PEG and P188 have a synergistic effect on cell fusion. We will test PEG/P188 on a neuroblastoma cell line to confirm this synergistic effect on cell fusion. We will also explore the P188/PEG combination in the in vivo experiment and determine whether the combination has a better nerve repair than other fusogens. We have tested PEG in the combination of triblock. These combinations did not produce higher fusion indices on L929 cells.

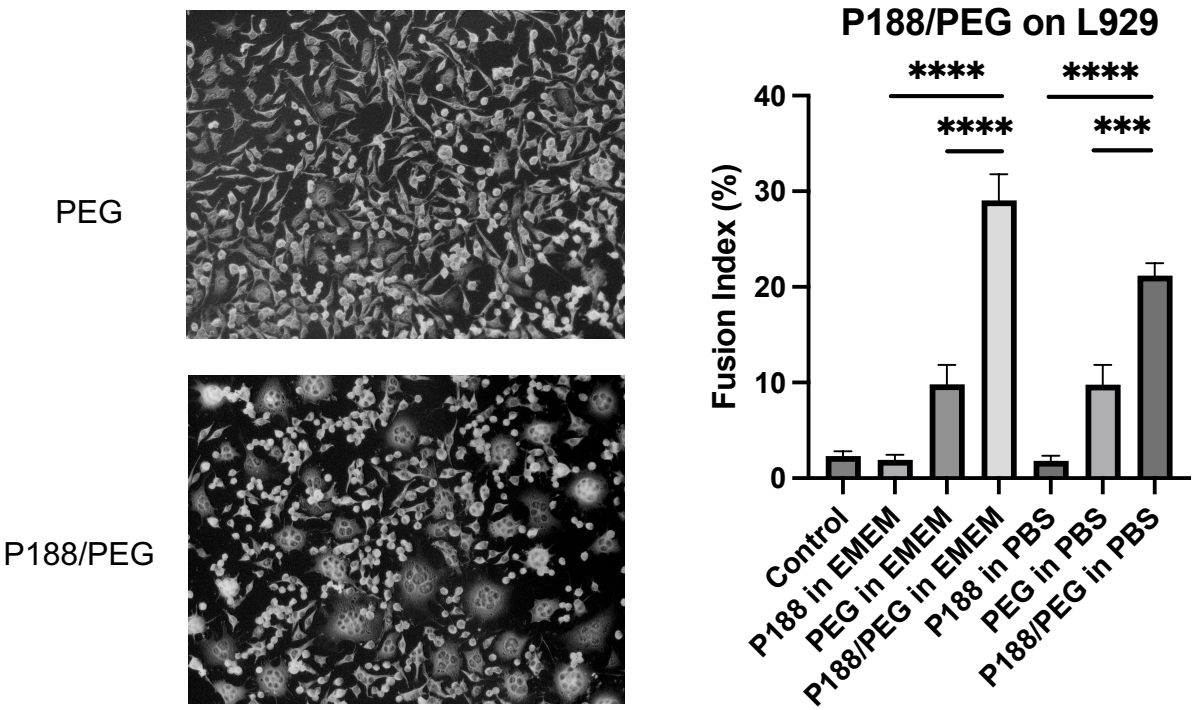

Figure 16. Cell fusion and fusion indices of PEG, P188, and P188/PEG treatment. PEG, P188, and P188/PEG were dissolved in either EMEM (growth media) or PBS and added to L929 cells for one minute. Cells were washed and cultured overnight before fixation and staining. The fusion index was defined by the total number of nuclei in fused cells divided by the total number of nuclei in all the cells. PEG and P188/PEG panels show L9292 cells after the treatment, where more fused cells can be observed in the P188/PEG treatment groups. P188/PEG treatment showed significantly higher fusion indices than the P188 and PEG treatments.

6.2. Determine the hemolytic activity of FNPs, TyPS, PEG and P188. A protocol for determining the effects of the fusogens on human red blood cells was developed and approved by Rutgers IACUC and submitted to the US Army Human Research Protection Office. To date, no experimental work has been performed on this Task.

Specific Aim 3: Evaluation of the lead FNP in an in vivo rat tibial nerve injury model.

Per the project Statement of Work, these in vivo studies were planned for Year 2. The experimental protocol was revised by our team and approved by ACURO in June, 2021. New electrophysiological recording equipment was purchased, however, due to still undiagnosed problems with the equipment, no animal studies were performed. Under the approval no-cost extension, the in vivo rat tibial nerve injury experiment will be performed in Year 4.

REFERENCES

1. Nardin C, Bolikal D, Kohn J, Nontoxic Block Copolymer Nanospheres: Design and Characterization. *Langmuir*. 2004;20(26):11721-11725. doi:10.1021/la0490285
2. Sheihet L, Dubin RA, Devore D, Kohn J, Hydrophobic Drug Delivery by Self-Assembling Triblock Copolymer-Derived Nanospheres. *Biomacromolecules*. 2005;6(5):2726-2731. doi:10.1021/bm050212u
3. Lima M, Le K-P, Kohn J, Devore D, Thermodynamic properties of tyrosine-derived diblock and triblock polymeric surfactants, manuscript in preparation.
4. Krevelen, D.W. van, and Klaas te Nijenhuis. Properties of Polymers: Their Correlation with Chemical Structure; Their Numerical Estimation and Prediction from Additive Group Contributions, Elsevier Science & Technology, 2009.
5. Grulke EA, Solubility Parameter Values, in Polymer Handbook, 3rd ed., Brandrup J, Immergut EH, eds., Wiley, New York, 1989.
6. Guo X, Rong Z, Ying X. Calculation of hydrophile–lipophile balance for polyethoxylated surfactants by group contribution method. *Journal of Colloid and Interface Science*. 2006;298(1):441-450. doi:10.1016/j.jcis.2005.12.009.
7. Kabanov AV, Nazarova IR, Astafieva IV, et al. Micelle Formation and Solubilization of Fluorescent Probes in Poly(oxyethylene-b-oxypropylene-b-oxyethylene) Solutions. *Macromolecules*. 1995;28(7):2303-2314. doi:10.1021/ma00111a026.
8. Aydin F, Chu X, Uppaladadium G, Devore D, Goyal R, Murthy NS, Zhang Z, Kohn J, Dutt Meenakshi, Self-Assembly and Critical Aggregation Concentration Measurements of ABA Triblock Copolymers with Varying B Block Types: Model Development, Prediction, and Validation. *The journal of physical chemistry B*. 2016;120(15):3666-3676. doi:10.1021/acs.jpcb.5b12594
9. Scholz N, Behnke T, Resch-Genger U, Determination of the Critical Micelle Concentration of Neutral and Ionic Surfactants with Fluorometry, Conductometry, and Surface Tension—A Method Comparison. *Journal of fluorescence*. 2018;28(1):465-476. doi:10.1007/s10895-018-2209-4.
10. Nagarajan R, Ganesh K, Comparison of Solubilization of Hydrocarbons in (PEO–PPO) Diblock versus (PEO–PPO–PEO) Triblock Copolymer Micelles. *Journal of colloid and interface science*. 1996;184(2):489-499. doi:10.1006/jcis.1996.0644.
11. Maskarinec S, Hannig J, Lee RC, Lee K, Yee C, Direct Observation of Poloxamer 188 Insertion into Lipid Monolayers. *Biophysical journal*. 2002;82(3):1453-1459. doi:10.1016/s0006-3495(02)75499-4.
12. Prescher H, Ling M, Lee RC, Copolymer Surfactant Poloxamer 188 Accelerates Post-axonotemetic Sciatic Nerve Regeneration. *Regenerative Engineering and Translational Medicine.* 2020. https://doi.org/10.1007/s40883-020-00174-y.
13. Davies JT, Rideal, EK, Interfacial Phenomena, Academic Press, New York, 1963, pp. 217-236.
14. Jurak M. Thermodynamic Aspects of Cholesterol Effect on Properties of Phospholipid Monolayers: Langmuir and Langmuir–Blodgett Monolayer Study. *J Phys Chem B*. 2013;117(13):3496-3502. doi:10.1021/jp401182c].
15. Deschênes L, Saint-Germain F, Lyklema J. Langmuir monolayers of non-ionic polymers: Equilibrium or metastability? Case study of PEO and its PPO–PEO diblock copolymers. *Journal of colloid and interface science*. 2015;449:494-505. doi:10.1016/j.jcis.2015.01.072
16. Ottico E, Prinetti A, Prioni S, Giannotta C, Basso L, Chigorno V, Sonnino S, Dynamics of membrane lipid domains in neuronal cells differentiated in culture. *Journal of lipid research*. 2003;44(11):2142-2151. doi:10.1194/jlr.m300247-jlr200

17. Hoffman A, Bamba R, Pollins A, Thayer WP, Analysis of polyethylene glycol (PEG) fusion in cultured neuroblastoma cells via flow cytometry: Techniques & optimization. *Journal of clinical neuroscience*. 2017;36:125-128. doi:10.1016/j.jocn.2016.10.032

What opportunities for training and professional development has the project provided?

- Mariana Lima was a graduate student in the Department of Chemistry and Chemical Biology at Rutgers University. Her thesis work on this project was guided by Prof. Joachim Kohn and Dr. David Devore. Mariana defended her thesis in August, 2021, and received a Doctorate in Chemistry. Dr. Lima then took a postdoctoral position with Prof. Kathryn Uhrich at the University of California, Riverside.

- Daniel Chakhalian, MD, was an NIH T-32 Postdoctoral Fellow who was mentored by Prof. Joachim Kohn at Rutgers University and Prof. Kacy Cullen at the University of Pennsylvania. Dr. Chakhalian was on leave from clinical programs for the purpose of professional development as a medical research scientist and physician and he returned to his clinical work in June, 2021.

- Cemile Bektas, PhD, was an NIH T-32 Postdoctoral Associate who was mentored by Prof. Joachim Kohn and Prof. Kibum Lee in the Department of Chemistry and Chemical Biology at Rutgers University. She contributed to this work in 2020 through 3D printing of the DRG scaffolds and in vitro DRG studies and moved to a new postdoctoral position with another laboratory in March, 2021.

- Dr. Joseph Rosen, Dartmouth Hancock Medical Center, visited Rutgers on July 16, 2021, and provided students at the Prof. Young's Keck Center with hands-on training in the surgical procedures required in this project for performing the electrophysiological studies of the repair of transected rat tibial and sciatic nerves.

How were the results disseminated to communities of interest?

- Dr. Mariana Lima gave an oral presentation, “Self-Assembly of Tunable Biodegradable Diblock and Triblock Polymeric Surfactants into Functional Nanoparticles,” at the American Chemical Society Annual Meeting on April 13, 2021; the co-authors were Kim-phuong Le, PhD, David I Devore, PhD and Joachim Kohn, PhD.

- Dr. Mariana Lima completed and submitted her thesis, Size Control of Self-Assembled Polymeric Nanospheres for Biomedical Applications, in August, 2021. A manuscript based on Dr. Lima’s thesis, co-authored by Prof. Joachim Kohn and Dr. David Devore, was submitted to the Journal of Colloid and Interface and is currently being revised for re-submission.

- Dr. Antonio Merolli gave a presentation at the Society of Biomaterials meeting in 2021, “Can polyethylene glycol be a trigger for a “side-by-side” axonal fusion mechanism?,” co-authored by Cemile Bektas, PhD, Robert Schultz,PhD, and Yong Mao, PhD.

- Dr. Antonio Merolli and Dr. Cemile Bektas co-authored a paper, “Hoechst 33342 as a marker for imaging neurites of Dorsal Root Ganglion in vitro (2021),” **J Anatom**, epub ahead of print.

What do you plan to do during the next reporting period to accomplish the goals?

In the Year 4 no-cost extension of this project, we will pursue in vitro demonstrations of the fusogenic activity of the TyPSs, P188 and PEG, using red blood cells and other eukaryotic cells already known to undergo fusion in the presence of PEG. We will then select candidate TyPSs and FNPs to start the in vivo rat tibial nerve transection experiments. If none of the first set of TyPS or FNPs with cholesterol, appear to provide a satisfactory combination of properties including low cytotoxicity and high fusogenic activity in vivo, then we will select from among a number of commercially available or readily synthesized block copolymers (e.g., other Poloxamers and polylactide triblocks) based on the observed relationships between our thermodynamic parameter calculations and our biophysical (e.g., Langmuir film) and cell culture data.

4. IMPACT:

What was the impact on the development of the principal discipline(s) of the project?

We are preparing additional manuscripts for publication which we anticipate will have a significant impact on the field, particularly if we can demonstrate that the TyPS or FNPs provide improved fusion compared to PEG for repair of transected rat nerves in vivo.

What was the impact on other disciplines?

This project is directed at the repair of peripheral nerve injuries. There is substantial published work which leads us to believe that the TyPS and TyPS/cholesterol FNPs have the potential to be effective in the repair and regeneration of spinal cord injuries. Prof's Wise Young and Dongming Sun at the W.M. Keck Center at Rutgers University are actively developing experimental plans to investigate this opportunity.

An Invention Disclosure has been submitted by Dr. David Devore and Prof. Joachim Kohn to Rutgers Innovation Ventures group for review. The disclosure covers compositions of matter and methods of use of the diverse polymeric surfactants such as the TyPS for cell surface modification including nerve fusion and repair. It is anticipated that a Provisional Patent based on this Invention Disclosure will be filed in the first quarter of 2022.

What was the impact on society beyond science and technology?

Nothing to report.

5. CHANGES/PROBLEMS:

Early in 2021, Rutgers University submitted for review/approval (per our Contract Terms and Conditions as delineated in the DoD Research General Award Terms and Conditions, FMS Article IV) a request for a change of Principal Investigator from Prof. Joachim Kohn to Prof. Wise Young. This request was put forth as Dr. Kohn retired from Rutgers with an effective date of November 1, 2020. Dr. Young subsequently received approval from the Department of Defense and has assumed the role of Principal Investigator of the project. Dongming Sun, MD, PhD, the Assistant Director of the W.M. Keck Center at Rutgers, has joined the project team and with Prof. Young has initiated work on the project's Tasks related to vitro cell culture and in vivo electrophysiology studies. Due to the closure of the Kohn Laboratory at Rutgers University, however, all of the students and postdoctoral fellows who contributed to the project had to find new positions and left the project team on or before August 2021. Dr. Antonio Merolli also left the project team on December 31, 2021, for a position in Rutgers' Physics Department.

Actual or anticipated problems or delays and actions or plans to resolve them

The closure of the Kohn Laboratory at Rutgers after Prof. Kohn's retirement, and the ongoing challenges of working during the COVID-19 pandemic, have resulted in substantial personnel turnover. Prof's Young and Sun are actively seeking to hire new personnel to continue the laboratory work. Although we have tried our best to organize the research team to achieve the project goals, we have encountered a long delay in finding and hiring new personnel. We hired a full-time technician in October 2022, and he has been involved in the project since. Dr. Joseph Rosen and Dr. David Devore will continue to have active consulting roles on the project in Year 4.

The dorsal root ganglia experiments have shown that axons retracted significantly following surgical blade transection and hence end-to-end fusion was not observed. It has also been difficult to conclusively demonstrate that significant side-to-side fusion of dorsal root ganglia axons occurs in the presence of PEG, Poloxamer 188 or the TyPSs. The mouse fibroblast cell line (L929) has been established to study cell fusion. We have used this cell line to screen TyPS and test P188 and PEG on cell fusion and obtained reliable results. An alternative in vitro cell culture experiments are now planned using rat neuroblastoma cells known to undergo significant fusion in the presence of PEG.

Changes that had a significant impact on expenditures

Personnel turnover has impacted the rate of expenditures on salaries, benefits and lab supplies.

Remaining funds will be utilized in the Year 4 project extension.

Significant changes in use or care of human subjects, vertebrate animals, biohazards, and/or select agents

Significant changes in use or care of human subjects
Nothing to report.

Significant changes in use or care of vertebrate animals
Nothing to report.

Significant changes in use of biohazards and/or select agents
Nothing to report.

6. PRODUCTS:

- **Publications, conference papers, and presentations**
  Journal publications.

  - Merolli A, Bektas C, "Hoechst 33342 as a marker for imaging neurites of Dorsal Root Ganglion in vitro (2021)," J Anatom, epub ahead of print.

  - Lima MRN, Devore DI, Kohn J, "Nanosphere size control by varying the ratio of copolymer blends," J Coll Int Sci (submitted and under revision).

  - Bektas C, Mao Y, Merolli A, "Refining the dorsal root ganglion in-vitro culture to better investigate the possible occurrence of vertebrate axonal fusion" Biomedicines (Major revision required)

  - Merolli A, Kasaei L, The role of conductivity in electrophysiological measurements of candidate molecules for vertebrate axonal fusion (in preparation)

  - Mariana R. N. Lima, Kim-Phuong N. Le, Daniel Chakhalian, Yong Mao, Joachim, Kohn, David I. Devore, "Diblock and Triblock Tyrosine-derived Polymeric

Surfactants as Cell Membrane Modifiers" Journal of Colloid and Interface Science (submitted and under revision).

Books or other non-periodical, one-time publications.

- Mariana Reis Nogueira de Lima, SIZE CONTROL OF SELF-ASSEMBLED POLYMERIC NANOSPHERES FOR BIOMEDICAL APPLICATIONS, A dissertation submitted to the School of Graduate Studies, Rutgers, The State University of New Jersey, August 31, 2021

Other publications, conference papers and presentations.

- Lima, MRN, Le K-P, Devore DI, Kohn JK, "Self-Assembly of Tunable Biodegradable Diblock and Triblock Polymeric Surfactants into Functional Nanoparticles," American Chemical Society Annual National Meeting, April 13, 2021

- Merolli A, Bektas C, Shultz R, Mao Y, meeting in 2021, "Can polyethylene glycol be a trigger for a "side-by-side" axonal fusion mechanism?," Society for Biomaterials Annual Meeting, April 20, 2021

- Antonio Merolli, Cemile Bektas, Yong Mao
  Poly-ethylene glycol might trigger a "side-by-side" axonal fusion mechanism in vertebrate DRG in-vitro
  American Society for Peripheral Nerve – Carlsbad 2022 (accepted: participation cancelled due to COVID restrictions)

- Antonio Merolli, Leila Kasaei, Leonard C. Feldman
  Helium-ion microscopy hints at a complex "side-by-side" PEG-fusion mechanism for DRG neurites
  Society for Biomaterials – Baltimore 2022 (submitted)

- **Website(s) or other Internet site(s)**

https://sites.rutgers.edu/lbr/peripheral-nerve-regeneration-and-treatment/

- **Technologies or techniques**

Tyrosine-derived polymeric surfactants are being developed in this project for fusion of transected peripheral nerves. Many other potential applications of these block copolymer surfactants are envisioned.

- **Inventions, patent applications, and/or licenses**

As stated above, an Invention Disclosure has been submitted by Dr. David Devore and Prof. Joachim Kohn to Rutgers Innovation Ventures group for review.

- **Other Products**

Nothing to report.

7. PARTICIPANTS & OTHER COLLABORATING ORGANIZATIONS

What individuals have worked on the project?

Name: Wise Young, MD, PhD
Project role: PI, Research
Researcher Identifier:
Person-months worked: 2.0
Contribution: Project leadership
Funding support: W.M. Keck Center, Rutgers University

Name: Dongming Sun, MD, PhD
Project role: Research
Researcher Identifier:
Person-months worked: 2.0
Contribution: In vitro cell culture and in vivo electrophysiology
Funding support: W.M. Keck Center, Rutgers University

Name: David I Devore, PhD
Project role: Consultant
Researcher Identifier:
Person-months worked: 3.0
Contribution: Thermodynamic calculations, project management, preparation of annual reports

Name: Joseph Rosen, MD
Project role: Consultant
Researcher Identifier:
Person-months worked:0.2
Contribution: Review of experiments, experimental planning, clinical perspectives

Name: Antonio Merolli, MD
Project role: Co-investigator
Researcher Identifier:
Person-months worked: 2.0
Contribution: Experimental planning, perform DRG experiments and data analysis, prepare for in vivo rat surgeries, clinical perspectives

Name: Yong Mao, PhD
Project role :Research (Research Associate Professor)
Researcher Identifier:
Person-months worked: 2.0
Contribution: Performed in vitro cytotoxicity experiments, experimental planning and data review
Funding support: NJ Center for Biomaterials, Rutgers University

Name: Daniel Chakhalian, MD
Project role: Research
Researcher Identifier:
Person-months worked: 6
Contribution: Flow cytometry experiments, clinical perspectives

Name: Joshua Sen, BA
Project role: Research
Researcher Identifier:
Person-months worked: 4
Contribution: Fusion index from cell culture

Funding support: NIH T-32 Fellowship Rutgers University

Name: Cemile Betkas, PhD
Project role: Research
Researcher Identifier:
Person-months worked: 2
Contribution: Design and fabrication of 3d printed scaffolds, dorsal root ganglia experiments
Funding support: NIH T-32 Fellowship, Rutgers University

Name: Kim-phuong Le, PhD
Project role: Research (Research Assistant Professor)
Researcher Identifier:
Person-months worked: 4
Contribution: Biophysical characterization of block copolymer surfactants

Name: Mariana Lima, BS
Project role: Research
Researcher Identifier:
Person-months worked: 8
Contribution: Design, synthesis and biophysical characterization of block copolymer surfactants

Name: Christine Gwin, BA
Project role: Research Technician
Researcher Identifier:
Person-months worked: 2
Contribution: Support of in vitro and in vivo experiments

Name: Robert Shultz, PhD
Project role: Research
Researcher Identifier:
Person-months worked: 1
Contribution: prepare dorsal root ganglia, experimental planning
Funding support: NIH T-32 Fellowship, University of Pennsylvania

Has there been a change in the active other support of the PD/PI(s) or senior/key personnel since the last reporting period?

Nothing to report.

What other organizations were involved as partners?

Organization: University of Pennsylvania
Location: Philadelphia, PA
Partner's contribution: Robert Shultz, PhD, a Rutgers T-32 program postdoctoral fellow working under the mentorship of Prof. Kacy Cullen at the University of Pennsylvania, actively participated in the project team meetings, providing valuable insights on nerve cell culture and fusogens, and he isolated and provided ex vivo rat dorsal root ganglia for the experiments at Rutgers.

8. SPECIAL REPORTING REQUIREMENTS

COLLABORATIVE AWARDS:

Nothing to report.

QUAD CHARTS:

The Quad Chard is attached below.

9. APPENDICES:

Appendix 1. Quad Chart

Award Log Number:PR192281 Award Title:W81XWH2010048/ Fusogen Nanomedicine for Peripheral Nerve Repair

PI: Wise Young, MD, PhD; Rutgers University, Piscataway, NJ **Budget:** $298,962

Topic Area: FY19 PRMRP Discovery Award **Mechanism:** Funding Opportunity

Research Area(s): SCS Coding 1400 Neuroscience **Award Status: January 1, 2020 –December 31, 2022**

Study Goals: The goal of this research project is to develop a new paradigm for the treatment of traumatic nerve injuries. A thermodynamically-based understanding of polymeric fusogen activity will emerge from the structure-activity relationships obtained here. The ultimate project deliverable will be a nanomedicine which restores motor and sensory function for trauma patients with severed and crushed peripheral nerves.

Specific Aims: Aim 1. Formulation and biophysical characterization of fusogen nanoparticles (FNPs) comprised of tyrosine-derived polymeric surfactants (TyPSs) designed and synthesized based on calculated thermodynamic properties; Aim 2. Evaluation of FNP in vitro axonal membrane repair and cytotoxicity; Aim 3. Evaluation of the lead FNP in an in vivo rat tibial nerve injury model.

Key Accomplishments and Outcomes: 1) Calculated thermodynamic solubility parameters and hydrophile; lipophile balances (HLBs) for a wide range of TyPSs, polyethylene glycol (PEG) and Poloxamer 188 correlated with their ability to bind cholesterol and to interact with cell phospholipids in Langmuir monolayer films; 2) Three A-B-A triblock and three A-B diblock TyPSs were synthesized based on their thermodynamic properties and were demonstrated to self-assemble into FNPs having particle diameters under 100nm, appropriate for injectable nanomedicines; 3) the most hydrophobic (lowest HLB) triblock TyPS was found to most strongly interact with Langmuir phospholipid monolayer films and its FNP provided controlled binding and release of significant levels of cholesterol; 4) the TyPSs were non-cytotoxic to human dermal cells and caused the fusion of rat B35 neuroblastoma cells while improving their viability; and, 5) methods developed to determine axonal fusion in rat dorsal root ganglia were not able to effectively determine the fusogenic potential of PEG or the TyPSs, and in vivo methods approved by the US Army ACURO will be pursued under a DoD-approved no-cost extension to obtain clear evidence of fusogen performance.

Publications: 1 PhD thesis; 1 journal article; 2 presentations at national meetings (Am.Chem.Soc.; Soc.Biomaterials)
Patents: 1 Invention Disclosure submitted to Rutgers Innovation Ventures for review
Funding Obtained: none to date

Appendix 2. Transition Plan Questionnaire

Directions: Please answer all questions that apply for each product under development. Please fill out one document per product.
This is not an application for funding; however, answers will help us understand the outcomes and products from your award.

1. After the award closes, would you be willing to periodically provide voluntary information (via email) regarding the project status (i.e. where the research is headed)? Yes ☑ or No ☐
These responses will help CDMRP demonstrate the return on its investments and will help demonstrate that the CDMRP is a responsible and successful steward of federal research funding.

2. What conclusion(s) does your final data support?

We have just completed Year 2 of our two year project. We have concluded from our work to date in Years 1and 2 that our tyrosine-derived polymeric surfactants (TyPSs) can be designed using calculated thermodynamic properties, specifically Hansen solubility parameters and Hydrophile:Lipophile Balance (HLB), such that they effectively self-assemble into fusogen nanoparticles (FNPs) with high binding affinity for cholesterol and they strongly insert into phospholipid film models of cell membranes. The TyPSs and FNPs improve the viability of human dermal cells and rat neuronal cells in vitro, and depending on their specific compositions, some cause in vitro fusion of the rat neuronal cells. It is anticipated that the observed in vitro fusogenicity of the FNPs will be observed in the planned in vivo rat tibial nerve transection studies to be determined in the DoD-approved Year 3 no-cost project extension.

3. Will you/have you applied for/obtained follow-on-funding for this project? If yes, please list (a) funding organization, (b) total budget requested/obtained, and (c) title of the funded proposal. ***This information will be recorded as an outcome to this award.***

Yes, we intend to seek follow-on funding and are awaiting completion of our initial in vivo rat model studies before determining the best opportunities (NIH R01 and/or DoD PRMRP funding).

4. What will be the next step(s) for this project?

Completion of key remaining Year 1 and Year 2 Tasks which were delayed due to the closure of the Kohn Laboratory at Rutgers as well as by the COVID-19 pandemic. The focus will be on demonstrating relative fusogen performance with in vitro cell cultures and then with in vivo rat sciatic nerve transection model studies.

5. How would you classify your lead candidate product? a
(a) Therapeutic (Small Molecule, Biologic, Cell/Gene Therapy): Please choose, if applicable
(b) Diagnostic
(c) Device
(d) Research Tool to Address a Research Bottleneck
(e) Knowledge Product (Non-material product such as a compound library, database, something that improves clinical practice, education, etc.)
(f) Other - Please Specify: NANOMEDICINE

6. How does your candidate product aid the Warfighter, Veteran, Beneficiary, and/or General Population?

Peripheral nerve injuries suffered in combat are a leading cause of unfitting conditions. The fusogen approach has the potential of making a paradigm shift in how these injuries are treated and in providing substantial improvements in the restoration of nerve function.

7. Therapy / Product Development, Transition Strategies, and Intellectual Property

Describe the steps and relevant strategies required to move the candidate product (knowledge or tangible) to the next phase of development and/or commercialization. Please address any issues with intellectual property.

PIs are encouraged to explore the technical requirements and the current regulatory strategies involved in product development as well as to work with their organization's Technology Transfer Office (or equivalent regulatory/legal office), federal/international regulatory experts, to develop the transition plan and to explore developing relationships with industry, DoD advanced developers (e.g. USAMMDA), and/or other funding agencies to facilitate moving the product into the next phase.

An Invention Disclosure has been submitted to the Rutgers University Innovation Ventures group and is under review for possible patent application filing. This is expected to lead to a Provisional patent application once the in vivo studies are completed. Assuming that the TyPS-based fusogenic nanoparticles (FNPSs) provide effective repair of transected rat tibial nerves in the experiments planned in Year 3, subsequent pre-clinical research will include large animal in vivo studies to determine FNP dosage-safety, biodistribution, pharmacokinetics and pharmacodynamics. In addition, a cGMP manufacturing process will be established. It is likely that an ongoing clinical trial of the fusgoenic efficacy of poly(ethylene glycol) (PEG) being led by another research group may be completed by that time and a decision can be made on whether to pursue FDA 510(K) approval for a TyPS product using either PEG or Poloxamer 188 as predicate devices, which would allow relatively rapid commercialization, or whether to use the FDA's new drug (Investigation New Drug, IND) pathway for a combination product of a TyPS-based FNP with encapsulated cholesterol. The IND pathway would require human clinical trials.